The geochemistry of modern calcareous barnacle shells and applications for palaeoenvironmental studies

Ullmann, C. V.; Gale, A. S.; Haggett, J.; Wray, D.; Frei, R.; Korte, C.; Broom-Fendley, S.; Littler, K.; Hesselbo, S. P.

Published in:
Geochimica et Cosmochimica Acta

DOI:
10.1016/j.gca.2018.09.010

Publication date:
2018

Document version
Publisher's PDF, also known as Version of record

Available online at www.sciencedirect.com

ScienceDirect

Geochimica et Cosmochimica Acta 243 (2018) 149–168

Geochimica et Cosmochimica Acta

www.elsevier.com/locate/gca

The geochemistry of modern calcareous barnacle shells and applications for palaeoenvironmental studies

C.V. Ullmann [a,*], A.S. Gale [b], J. Huggett [c], D. Wray [d], R. Frei [e], C. Korte [e], S. Broom-Fendley [a], K. Littler [a], S.P. Hesselbo [a]

[a] University of Exeter, Camborne School of Mines and Environment and Sustainability Institute, Treliever Road, Penryn TR10 9FE, UK
[b] University of Portsmouth, School of Earth and Environmental Sciences, Burnaby Building, Burnaby Road, Portsmouth PO1 3QL, UK
[c] Petroclays, The Oast House, Sandy Cross Lane, Heathfield, Sussex TN21 8QP, UK
[d] University of Greenwich, School of Science, Pembroke, Chatham Maritime, Kent ME4 4TB, UK
[e] University of Copenhagen, Department of Geosciences and Natural Resource Management, Øster Voldgade 10, 1350 Copenhagen, Denmark

Received 14 March 2018; accepted in revised form 12 September 2018; available online 22 September 2018

Abstract

Thoracican barnacles of the Superorder Thoracicalcarea Gale, 2016 are sessile calcifiers which are ubiquitous in the intertidal zone and present from very shallow to the deepest marine environments; they also live as epiplankton on animals and detritus. The geochemical composition of their shell calcite has been shown to yield information about environmental conditions, but comprehensive analyses of barnacle shell geochemistry are so far lacking.

Here, a dataset is reported for Mg/Ca, Sr/Ca, Mn/Ca, Fe/Ca, as well as carbon and oxygen isotope ratios for 42 species from the Balaniformes, Verruciformes, Scalpelliformes and Lepadiformes. Barnacles predominantly form low-Mg-calcite with very high Sr/Ca ratios averaging 4.2 mmol/mol. The Mn/Ca and Fe/Ca ratios in shell plates are variable and can exceed >4 mmol/mol in barnacles that are attached to manmade structures or live close to (anthropogenic) sources of Mn and Fe. No strong phylogenetic control on the average element/Ca ratios is observed in barnacles. The Balaniformes show a ca. 40% enrichment of Mg in their scuta and terga as compared to other shell plates—a pattern which is not seen in other barnacles. The combination of low to medium Mg/Ca ratios and high Sr/Ca ratios is rare for marine biogenic calcite. Barnacles may thus become important for robustly reconstructing past seawater composition, if this signature is also present in fossil barnacle calcite and can be used alongside other fossil taxa with different Sr incorporation behaviour.

Carbon and oxygen isotope data support the view that the oxygen isotope thermometer for barnacles is robust and that most barnacle species form their calcite near isotopic equilibrium with ambient water. The Lepadiformes, however, show a tendency for strong co-variation of $\delta^{13}C$ with $\delta^{18}O$ values and depletion in ^{13}C and ^{18}O which is attributed to isotopic disequilibrium during shell secretion.

Strong systematic fluctuations in Mg/Ca ratios over length scales of ca. 5–15 μm are exhibited by the scalpelliform species *Capitulum mitella*, the only studied species which consistently forms high Mg calcite, and are tentatively linked to tidal control on the shell secretion pattern. Cathodoluminescence images for this species suggest that additionally a seasonal pattern of Mn distribution in its shell plates is recorded, pointing to a potential use for reconstruction of seasonal changes in terrestrial element supply.

Keywords: Barnacle; Biomineral; Carbon isotopes; Oxygen isotopes; Trace elements

* Corresponding author.
E-mail address: C.v.ullmann@gmx.net (C.V. Ullmann).

https://doi.org/10.1016/j.gca.2018.09.010
0016-7037/

1. INTRODUCTION

Barnacles have been of long-standing scientific interest with detailed work on taxonomy and fossil forms reaching back to Charles Darwin (e.g., Darwin, 1851, 1854). Thoracican barnacles (subclass Cirripedia) first appeared in the Early Paleozoic (Briggs et al., 2005; Pérez-Losada et al., 2008) and developed shells of phosphatic composition (Gale and Schweigert, 2016). This basal clade is represented by the living genus *Ibla*, which has shell plates composed of a poorly ordered hydrogen-phosphate-like material (Reid et al., 2012). Thoracicans evolved shells of calcite in the Jurassic, and form a monophyletic clade called the Thoracicalcarea Gale (2016), which are abundant in the World's oceans today. Calcareous barnacles first appeared in the Bathonian (mid-Jurassic), and by the end of the Jurassic (Tithonian) forms referred to the family Zeugmatolepadidae were abundant and widespread, mostly as epifauna attached to ammonite shells and driftwood (Gale, 2014, in press). In the Lower Cretaceous (Aptian) stalked benthonic cirripedes of the extant families Calanticidae and Scalpellidae appeared, which persist in deeper marine habitats to the present day (Gale, 2015). One group of stalked calcareous barnacles became epiplanktonic (lepadomorphs). Calcareous cirripedes first adapted to shallow marine hard substrates in the Late Cretaceous (Gale and Sørensen, 2015) and neobalanomorphs appeared in the Paleogene. These radiated rapidly, and by the Miocene these sessile forms were globally abundant and locally rock-forming in shallow marine habitats. Today they occupy a wide range of habitats from the intertidal zone down to deep sea trenches in the modern oceans (Foster, 1987).

Calcareous barnacles secrete their shells onto a chitinous cuticle in a succession of very thin layers in synchronicity with the tidal cycle (Bourget, 1987) or endogenous semidiurnal rhythm (Bourget and Crisp, 1975). The thin layers are composed of polycrystalline calcite crystals enveloped in organic macromolecules (Gal et al., 2015) and show hierarchical patterns. These hierarchical patterns relate to seasonal changes in growth rate and decreasing band with throughout ontogeny modulating the thickness of growth bands (Bourget and Crisp, 1975). After an initial planktic life stage, barnacles settle in their final larval stage and become sessile (Shanks, 1986), recording environmental conditions at their growth site during their adult life. Particular interest has been focussed on their attachment to various surfaces due to the negative economic impact of barnacle fouling (e.g., Christie and Dalley, 1987; Swain et al., 1998). The shells of barnacles have, however, also found use in ecological and environmental studies: $\delta^{13}C$ and $\delta^{18}O$ values of turtle and whale barnacles have been employed to trace the movement patterns of their host animals (Killingley, 1980; Killingley and Lutcavage, 1983) and a barnacle oxygen isotope thermometer has been established (Killingley and Newman, 1982). This barnacle thermometer has, for example, been employed in determining habitats of turtle barnacles (Detjen et al., 2015), and deciphering the point of origin of museum specimens (Newman and Killingley, 1985). Additionally, carbon isotope ratios in body tissues of intertidal barnacles have been identified as a potential proxy for habitat elevation with respect to the tidal level (Craven et al., 2008).

Element/Ca ratios of barnacle shells have been studied and proposed as tracers of salinity (Gordon et al., 1970) and shore level (Pilkey and Harriss, 1966; Bourget, 1974). Significant inter-specimen differences in shell composition across different localities have additionally been identified as fingerprinting tool to locate harvest points of edible goose barnacles (Albuquerque et al., 2016). Despite such encouraging studies, not much is known about the chemical composition of barnacle shell material, and compilations of barnacle shell chemistry rely on very few samples (Chave, 1954; Dodd, 1967).

From the few available data it has been noted that barnacle shell calcite is dissimilar from most commonly studied biogenic calcite as its very high Sr concentrations mean it plots off a proposed correlation line of Sr versus Mg content (Carpenter and Lohmann, 1992). Whether barnacles carry any species-specific element signatures and whether there are differences in element concentrations in their shell plates has, however, not been comprehensively addressed (but see Iglikowska et al., 2018a).

Here we present $\delta^{13}C$ and $\delta^{18}O$ values as well as Mg/Ca, Sr/Ca, Mn/Ca and Fe/Ca ratios of 42 modern barnacle species of the Lepadiformes, Scalpelliformes, Verruciformes and Balaniformes (see Pérez-Losada et al., 2008 for taxonomic scheme), constituting the first large survey of shell geochemistry in cirripedes. These analyses are complemented by XRD analyses of 27 specimens to confirm the calcitic nature of the shell material. We compare the geochemical signatures of the shells with environmental parameters and evaluate taxonomic trends in shell composition. Furthermore, we investigate intra-shell chemical variability to address overall compositional heterogeneity and plate-specific chemical fingerprints.

2. MATERIALS AND METHODS

Specimens from 47 sites, comprising 42 cirripede species of the Balaniformes, Lepadiformes, Scalpelliformes and Verruciformes (Fig. 1) from personal and museum

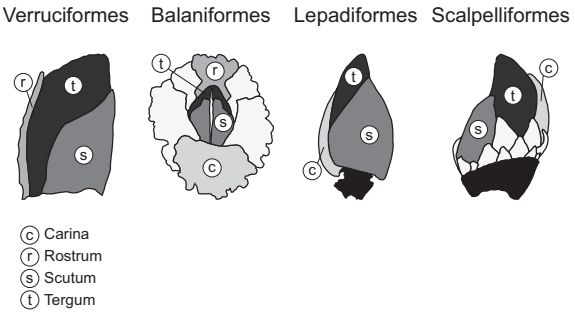

Fig. 1. Plate arrangements and general morphology of the four studied barnacle groups. Drawings are in right lateral view for Verruciformes, plan view for Balaniformes, left lateral view for Lepadiformes, and right lateral view for Scalpelliformes. All shown plates other than scuta and terga are considered as "wall plates" for the purpose of this study.

collections, were analysed (Table 1, Supplementary Fig. 1). Often only one specimen or part of one specimen was available for analysis, but in 15 cases several or multiple specimens from one locality could be studied (Table 1). Most of the specimens were preserved in alcohol, but specimens of samples 1, 3, 5, 16, 28, 36, 38, 39 and 46 were stored dried. Collection dates range from the 18th century to 2014. No effect of sample storage and specimen age has been observed in isotopic or element data. The samples cover a wide range of latitudes (75°N to 45°S; Fig. 2) and water depths from the intertidal zone to deep marine settings of approx. 2600 m water depth.

All specimens were transferred into separate beakers and reacted with 5% NaClO for at least 24 h to remove organic matter. The specimens were then rinsed multiple times with de-ionized water and residual organic matter was removed with stainless steel scalpel and tweezer. The cleaned shell plates were left to dry at room temperature. Samples for geochemical analyses were taken using a handheld drill with a drill bit of ca. 1 mm diameter or, where shell plates weighed 5 mg or less, by powdering entire shell plates with an agate pestle and mortar. Between 0.4 and 10 mg of powder per sample (usually 1–3 mg) were prepared and split into subsamples for isotope and element analysis. Typically ten $\delta^{13}C$ and $\delta^{18}O$ analyses per specimen were conducted (473 analyses in total), alongside 10–40 analyses of Mg/Ca, Sr/Ca, Mn/Ca and Fe/Ca ratios (1138 analyses in total; Supplementary Table 1).

2.1. Carbon and oxygen isotope ratio measurements

Isotope analyses were carried out at the Department of Geosciences and Natural Resource Management (IGN), University of Copenhagen. Samples 858–2045 (Supplementary Table 1) were analysed using a Delta V gas source isotope ratio mass spectrometer coupled with a Kiel IV device; and samples 2046–2681 (Supplementary Table 1) using an IsoPrime in continuous flow configuration.

Analyses using the Delta V were undertaken using ca. 50 µg of calcite powder. Batches of 40 vials, 30 samples and 10 standards comprising NBS-18, NBS-19 and an in-house standard (LM: Laaser Marble, Freie Universität Berlin, $\delta^{13}C = +1.51‰$ V-PDB, $\delta^{18}O = -5.17‰$ V-PDB), were measured. The accuracy of the runs was checked by multiple measurements of these standards. No isotopic adjustments of the raw data were made as analytical results of NBS-18 ($n = 19$), NBS-19 ($n = 20$) and LM ($n = 28$) conformed to certified or accepted values within measurement uncertainty. Reproducibility of multiple standard measurements was better than 0.07‰ (2 sd) for carbon isotope ratios for all standards, better than 0.15‰ (2 sd) for oxygen for NBS-19 and LM and 0.20‰ for NBS-18, which is known to be isotopically heterogeneous at the analysed weight scale (Ishimura et al., 2008).

For analyses using the IsoPrime, typically around 500 µg of calcite were measured. Samples were placed in sealed glass vials, flushed with He and reacted with ca. 50 µl of nominally anhydrous H_3PO_4 (~102%). Weight-dependent mass discrimination was corrected by multiple analyses of the in-house standard LEO (Carrara Marble, $\delta^{13}C = +1.96‰$ V-PDB, $\delta^{18}O = -1.93‰$ V-PDB) covering the entire weight range of samples. The accuracy of the analyses was controlled by periodic analysis of international standards (see Ullmann et al., 2013a). Reproducibility was checked by multiple measurements of LEO in every run ($n = 182$) and was 0.08‰ (2 sd) for carbon and 0.17‰ (2 sd) for oxygen isotope ratios over the course of the measurements.

2.2. Element/Ca ratio measurements

Element/Ca ratios were measured using a Perkin Elmer Optima 7000 DV ICP OES at IGN, University of Copenhagen. Typically ca. 500 µg of calcite powder were dissolved at a ratio of 1.5 ml of 2% HNO_3 per 100 µg of calcite powder to achieve a Ca concentration of ca. 25 µg/g. Batches of 120 samples were run together with 12 interspersed samples of JLs-1 (Imai et al., 1996) for control of accuracy and precision. Signal quantification was done using a four-point calibration with a blank solution, and three synthetic, matrix-matched solutions made up from single-element solutions. Average measured ratios of JLs-1 (2 sd, $n = 235$) are 14.0 ± 0.4 mmol/mol for Mg/Ca, 0.35 ± 0.01 mmol/mol for Sr/Ca, 0.03 ± 0.01 mmol/mol for Mn/Ca, and 0.07 ± 0.05 mmol/mol for Fe/Ca. Large relative uncertainty of the Mn/Ca and Fe/Ca analyses of JLs-1 is related to low Mn and Fe concentrations in this standard. The concentrations are near the limit of quantification for the method which are 0.01 mmol/mol for Mn and 0.05 mmol/mol for Fe.

2.3. XRD analysis

For XRD analysis at the University of Greenwich, shell plates were ground to a powder in a Tema mill (using industrial methylated spirits to minimise structural grinding damage). A few drops of the resulting slurry were allowed to dry on a silicon wafer. The powders were scanned on a Siemens PSD X-ray diffractometer using Ni-filtered Cu (Kα) radiation with a 0.02° step width, and 0.2 mm slits, from 5 to 70° 2ϑ. The data have been quantified using Macdiff 4.26 (http://www.geol-pal.uni-frankfurt.de/Staff/Homepages/Petschick/MacDiff/MacDiffInfoE.html) to deconvolute and measure peak areas.

2.4. High-resolution analysis of *Capitulum mitella*

The carina of the specimen of *Capitulum mitella* was set in a circular resin block of 25 mm diameter, glued to a glass slide, cut and polished to expose a section perpendicular to the growth increments at the maximum thickness of the plate.

2.4.1. Cathodoluminescence microscopy

The section was studied using a cathodoluminescence (CL) microscope with a Citl Mk-3a electron source at the University of Exeter, Camborne School of Mines. Operation conditions were approximately 350 µA and 18 kV. Photographs were taken using a Nikon digital camera with 4 second exposure time. A CL map of the entire section was

Table 1
Taxonomic and locality information as well as number of analysed specimens for studied barnacles (see also Supplementary Fig. 1). Samples for which XRD data were acquired are marked with a "y". Latitudes and longitudes are approximated from locality description where possible.

Number	Species name	Order	Locality	specimens	XRD	Latitude	Longitude	Water depth	Collection year
1	*Dosima exoleta*	Lepadiformes	Donegal, Ireland, pelagic - washed ashore	1	y	54°37′ N	8°10′ W		2008
2	*Dosima fascicularis*	Lepadiformes	Gammel Skagen beach; N Jutland, Denmark	1		57°53′ N	10°31′ E		2012
3	*Lepas anatifera*	Lepadiformes	Dorset, UK	3	y	50°N	2°W	floating wood	2010
4	*Lepas anserifera*	Lepadiformes	scraped off ship keel in Sydney, Australia	1					1951
5	*Lepas pectinata*	Lepadiformes	Paphos, Cyprus, attached to drift wood	2	y	34°50′ N	32°20′ E	floating wood	2014
6	*Calantica spinosa*	Scalpelliformes	New Zealand	1	y			intertidal	
7	*Calantica villosa*	Scalpelliformes	New Zealand	1	y			intertidal	
8	*Capitulum mitella*	Scalpelliformes	Hong Kong, attached to wood	1	y	22°N	114°E	intertidal	
9	*Pollicipes polymerus*	Scalpelliformes	Spain, W coast	1	y	42°N	9°W	intertidal	1995
10	*Amigdoscalpellum* sp.	Scalpelliformes	Arabian Sea	1	y			1108	
11	*Amigdoscalpellum rigidum*	Scalpelliformes	Porcupine Bight	1	y			2750	
12	*Arcoscalpellum sociabile*	Scalpelliformes	Cape Nomamisaki, Japan	1	y	31°N	130°E	220	
13	*Neoscalpellum* sp.	Scalpelliformes	Porcupine Bight	1	y			484	
14	*Scalpellum scalpellum*	Scalpelliformes	North Sea	1	y			subtidal	
15	*Scalpellum stearnsi*	Scalpelliformes	Cape Nomamisaki, Japan	1	y	31°N	130°E	220	
16	*Solidobalanus falax*	Balaniformes	Devon, UK	2	y	50°N	3°W	10	
17	*Striatobalanus amaryllis*	Balaniformes	Persian Gulf, 6 sea miles NE of Bahrain	1		26°20 N	50°45′ E	20	1938
18	*Striatobalanus amaryllis*	Balaniformes	Singapore, shallow water	1		1°10′ N	103°50′ E		1910
19	*Semibalanus balanoides*	Balaniformes	Havneby Havn, Rømø, Denmark	multiple		55°05′ N	8°33′ E	0	1978
20	*Semibalanus balanoides*	Balaniformes	Qaqortoq, Greenland	2		60°43′ N	46°02 W		1974
21	*Semibalanus balanoides*	Balaniformes	Seyðisfjörður, Iceland	1		65°16′ N	14°00′ W		1900
22	*Amphibalanus amphitrite*	Balaniformes	Banjul, Gambia, 6 foot scrapings off ship "Atlantide"	multiple					1945
23	*Amphibalanus eburneus*	Balaniformes	Navy Port, Cartagena, Colombia	1		10°24′ N	75°32′ W		1973
24	*Amphibalanus improvisus*	Balaniformes	Kristianhavns Voldgrav, Copenhagen, Denmark	4		55°40′ N	12°35′ E		1898
25	*Amphibalanus improvisus*	Balaniformes	ponton off Skovshoved havn, Copenhagen, Denmark	4		55°45′ N	12°36′ E		1958
26	*Amphibalanus variegatus*	Balaniformes	East of Singapore	multiple		1°20′ N	104°05′ E	10	1951
27	*Balanus balanus*	Balaniformes	Spitsbergen, Norway	1		78° N	15° E		2013
28	*Balanus concavus*	Balaniformes	UK, Isle of Wight	multiple	y	50°N	1°W	intertidal	2013
29	*Balanus crenatus*	Balaniformes	Dodds Narrows, Vancouver Isl., B.C., Canada	2		49°08′ N	123°50′ W	0	1915
30	*Balanus trigonus*	Balaniformes	Ambon Island, Indonesia	1		3°41′ S	148°10′ E	0	1922
31	*Megabalanus* sp.	Balaniformes	SE Asia	1	y				
32	*Megabalanus tintinnabulum*	Balaniformes	SE India	1					pre 1800 (?)
33	*Notomegabalanus algicola*	Balaniformes	Walvis Bay S Africa	1		22°56′ S	14°29′ E		1950
34	*Eochionelasmus ohtai*	Balaniformes	North Fiji Trench, Pacific	1	y	17°S	175°E	1990	
35	*Catomerus polymerus*	Balaniformes	SW Australia	1	y			intertidal	
36	*Chamaesipho columna*	Balaniformes	New Zealand	2	y			intertidal	
37	*Chthamalus fragilis*	Balaniformes	Mole near Fort Macon, Beaufort, N.C., USA	5		34°41′ N	76°40′ W		1972
38	*Chelonibia patula*	Balaniformes	Florida Keys, Florida, USA; attached to *Limulus*	1	y	24°N	81°W		
39	*Chelonibia* sp.	Balaniformes	Philippines, turtle barnacle	1	y				
40	*Coronula diadema*	Balaniformes	unknown, whale barnacle	1	y				
41	*Coronula diadema*	Balaniformes	sent from Julianehaab, Greenland	1					
42	*Bathylasma hirsutum*	Balaniformes	Porcupine Bight	1	y				

43	*Tesseropora sp.*	Balaniformes	New Zealand	1	y	23°N	120°E	intertidal	
44	*Tetraclitella japonica*	Balaniformes	Taiwan	1	y	5°37′ S	132°44′ E	intertidal	1922
45	*Yamaguchiella coerulescens*	Balaniformes	Kai Islands, Indonesia	2		54°37′ N	8°10′ W	just subtidal	2012
46	*Verruca stroemia*	Verruciformes	Donegal, Ireland, attached to Laminaria holdfast	1	y	25°S	70°E	2600	1987
47	*Metaverruca recta*	Verruciformes	Rodrigues Ridge, Indian Ocean	1	y				

made using a 2.5× magnification objective and a high-resolution trace approximately parallel to the growth direction was photographed using a 10× magnification objective yielding a nominal resolution of 0.32 μm per pixel. For the high-resolution trace, six images of the same frame were taken. The acquired RGB data were reduced to grayscale and all images combined by signal addition into a single file using image editing software to enhance the signal to noise ratio. Single frames were then overlaid and blended into a single image and the grayscale levels adjusted to yield the full spread from black to white without saturation. In the resulting CL mosaic, a series of eight bands of 10 pixel thickness and lengths from 2290 to 11,075 pixels were defined perpendicular to the growth increments of the shell plate. These bands were then cropped from the merged profile and grayscale information extracted using the Profile function of ImageJ software. Grayscale data for single bands were then merged into a single trace using distinct marker bands in overlapping areas. Where necessary, offsets in grayscale values, due to lateral offsets in the band position, were smoothed over a range of 100 μm around the marker band that defined the correlation point for the profiles. The resulting stacked profile corresponds to approximately 14.3 mm and 44,790 points.

2.4.2. Scanning electron microscopy and EDS scans

An electron dispersive X-ray map of relative Mg concentration in a ca. 850 × 850 μm frame with nominal resolution of 0.78 μm per pixel was generated for the same specimen using a FEI Field Emission Gun Scanning Electron Microscope at the University of Exeter, Environment and Sustainability Institute. Data were quantified using a double EDS detector setup for ca. 16 h in continuous scanning mode at 10 kV and a working distance of 12.9 mm. Line scans of ca. 800 μm long segments perpendicular to the growth increments through the entire section quantifying Ca (Kα) and Mg (K) were acquired with a nominal resolution of 1 μm per step. Integration time per pixel reading was set to 32 milliseconds and the line repeatedly scanned until cumulative integration times of 5 s per pixel were reached. Raw count rates were converted into count ratios of Mg/Ca to account for lateral signal variation and resulting traces overlaid and merged into a consecutive trace through the shell plate. Working distance, acceleration voltage and magnification were the same as for the element mapping. Secondary electron images at 400 nm per pixel resolution (850 μm × 850 μm frame size, 4.5–9 min integration time) were acquired for each line scan covering the entire trace to aid the correlation. The stack of 18 segments corresponds to c. 13.6 mm length, and was measured close to, but not exactly coincident with the CL trace.

3. RESULTS

Calcite was the only carbonate polymorph detected during XRD analyses of the barnacle specimens (Supplementary Fig. 2). Geochemical and isotopic effects potentially arising from other carbonate polymorphs, in particular aragonite (Bourget, 1987), are therefore not considered in the following.

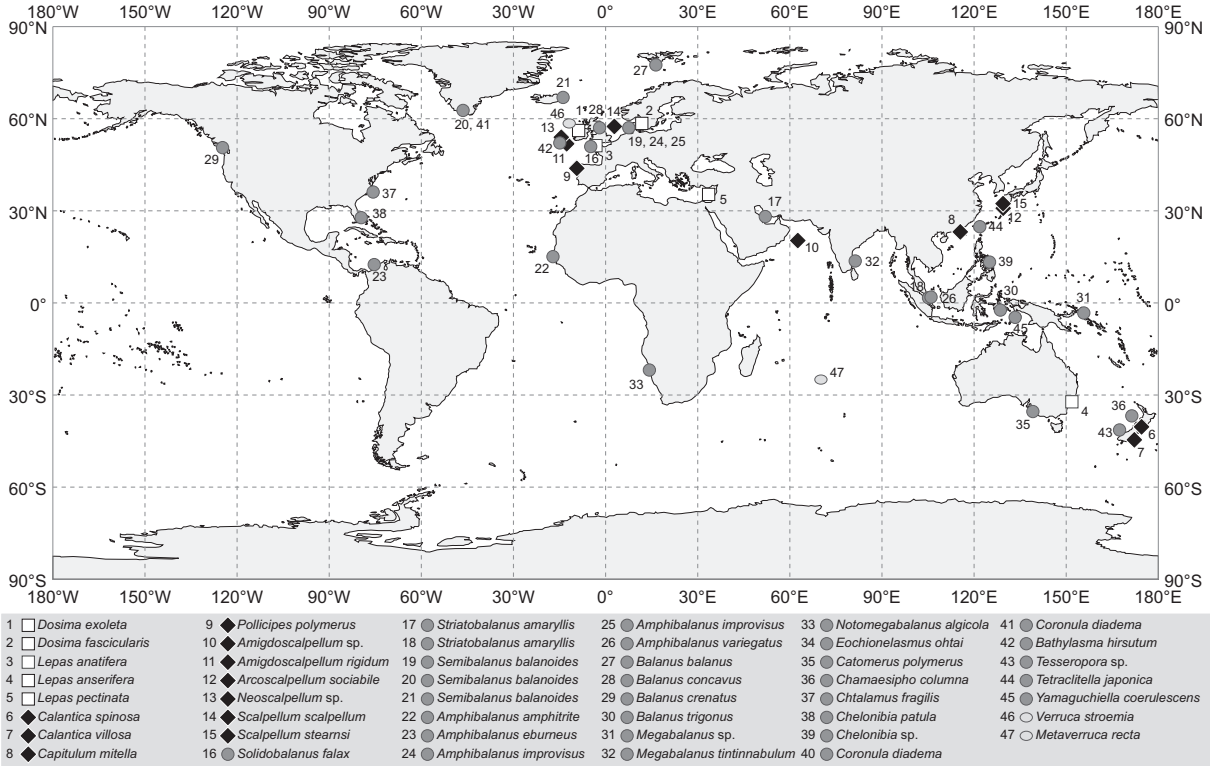

Fig. 2. Sample localities for the species studied here. White squares: Lepadiformes; black diamonds: Scalpelliformes; gray circles: Balaniformes; light gray ellipses: Verruciformes. Positions on the map are approximations, unless exact collection point is known (conf. Table 1).

3.1. Mg/Ca and Sr/Ca ratios

A wide range of Mg/Ca ratios of 4.0–132 mmol/mol is encountered in the analysed barnacle species (Supplementary Table 1). The vast majority of the samples can be classified as Low Mg Calcite (LMC) with 95% of the measured Mg/Ca ratios below 50 mmol/mol. Only the scalpelliform barnacle *Capitulum mitella* shows Mg/Ca ratios consistently in the field of high Mg calcite (HMC) (Fig. 3; Supplementary Table 1).

Interquartile (25–75%) ranges of Mg/Ca vary between 5% (*Scalpellum stearnsi*) and 72% (*Chelonibia* sp.), but typically 10–30% around the median value. Variability of the Mg/Ca ratios is, on average, larger in balaniform barnacles than in lepadiform, scalpelliform and verruciform barnacles. Median Mg/Ca ratios of four species observed at several localities show considerable intra-species differences of 16–32% (2 rsd). These differences are independent from distances between the localities. At single localities, however, Mg/Ca ratios of three *Lepas anatifera* specimens (UK) and wall plates of two *Semibalanus balanoides* specimens (Greenland) agree within 8% (2 rsd).

Sr/Ca ratios in the barnacle calcite range from 2.6 to 5.9 mmol/mol (Fig. 3), with median values of single species ranging from 2.7 to 5.2 mmol/mol. No clear correlation of Sr with Mg is noted ($r^2 = 0.09$ for median values). Within single barnacle specimens from a given locality, Sr/Ca ratios are comparatively stable, with interquartile ranges varying between 1% (*Scalpellum stearnsi*) and 15% (*Capitulum mitella*), but typically 4–10% around the median value. Median Sr/Ca ratios of four species observed at several localities also show only small relative differences of 1–13% (2 rsd), suggesting that median Sr/Ca ratios are robustly defined for the species presented here.

No clear distinctions of Mg/Ca ratios or Sr/Ca ratios between different barnacle orders are observed (Fig. 3).

3.2. Mn/Ca and Fe/Ca ratios

A wide range of Mn/Ca (detection limit to 4.1 mmol/mol) and Fe/Ca ratios (detection limit to 6.2 mmol/mol) is observed, but most species show low Mn and Fe levels (Fig. 4). Only specimens from two species exhibit median Mn/Ca ratios > 1 mmol/mol (*Semibalanus balanoides*; *Amphibalanus improvisus*) and the median for all specimens is 0.04 mmol/mol. Median Fe/Ca ratios above > 1 mmol/mol are also limited to two species (*Scalpellum stearnsi*, *Amphibalanus amphitrite*) and the median for all specimens is 0.05 mmol/mol.

Specimens with substantial amounts of Mn and/or Fe in the shell material (Fig. 4) mostly stem from very near shore localities or man-made structures: *S. balanoides* (median Mn/Ca = 2.7 mmol/mol) from a harbour on the Danish island Rømø; *A. improvisus* (median Mn/Ca = 1.2 mmol/mol) from Central Copenhagen, Denmark; *A. Amphitrite* (median Fe/Ca = 1.8 mmol/mol) scraped off a vessel in

Banjul, Gambia; *S. stearnsi* (median Fe/Ca = 1.1 mmol/mol) from Cape Nomamisaki, Japan.

A species control on Mn or Fe concentrations in shell calcite is not apparent as Mn and Fe concentrations across multiple specimens of the same species typically differ by an order of magnitude. Multiple specimens of the same species at a given locality, however, show closely matching Mn/Ca and Fe/Ca ratios as observed in three specimens of *Lepas anatifera* from Dorset, UK (Supplementary Table 1).

3.3. High resolution element distribution in *Capitulum mitella*

The consistently Mg-enriched nature of the calcite of *Capitulum mitella* means it is possible to study the high-resolution distribution of this element in its plates using electron beam techniques. Using Cathodoluminescence (CL) microscopy the Mg distribution pattern can furthermore be compared to qualitative Mn concentration maps at high spatial resolution.

SEM mapping and line scans of Mg distribution in *C. mitella* visualize prominent differences in Mg content visible already using backscatter electron imaging (Figs. 5 and 6). These strong fluctuations of Mg/Ca ratios from 0.13 to 0.45 cps/cps for large parts of the measured transect show clear peaks and troughs at a spacing of c. 5–15 μm (Supplementary Table 2). A rough conversion of raw Mg/Ca count rates from energy dispersive spectrometers into Mg/Ca ratios was attempted using the median Mg/Ca ratio from

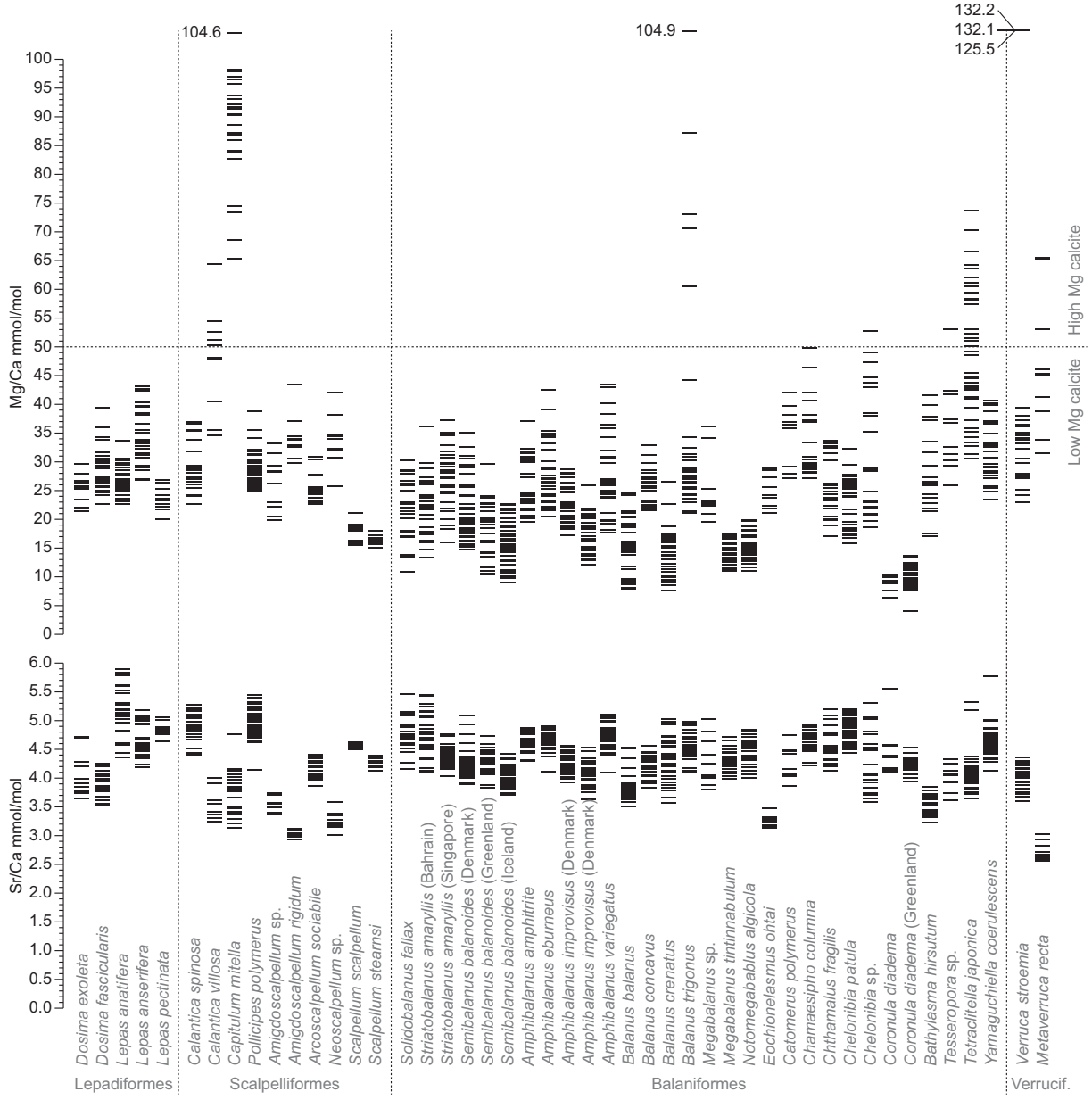

Fig. 3. Sr/Ca and Mg/Ca ratios measured for the barnacles from 47 localities (see also Supplementary Table 1).

ICP-OES measurements and assuming a similar mean value for the line scans as well as a linear detector response (Fig. 6). If this approximation is reasonably accurate, *C. mitella* secretes calcite with Mg/Ca ratio changes of 20–70 mmol/mol across a distance of a few micrometres, oscillating from nearly LMC to HMC.

CL mapping reveals a hierarchical banding structure in *C. mitella* (Fig. 5; Supplementary Table 3). This comprises a set of c. ten zones, starting with more luminescent bands separated by narrower, commonly quite prominent, zones of weak luminescence (Fig. 5). A multitude of thin luminescent bands occurs within the broad zones. The distance between the small-scale luminescent bands is the same as the distance between Mg/Ca peaks; detailed matching of CL and Mg signals in the area for which the Mg map was generated indicates that Mg-rich bands correspond to luminescent bands, even though peak intensities are dissimilar in detail (Fig. 6A). In order to quantify the peak match, both signals were de-trended and normalized and peaks of the CL profile matched against the Mg/Ca profile. Mg/Ca peaks were assigned if the signal showed a spike of at least 1 standard deviation amplitude in the normalized curve. A robust match was assigned for a CL peak if a spike with at least 1 standard deviation amplitude peaking within 1 µm was found. A tentative match was assigned where the CL signal peaked within 2 µm of the Mg peak, or the amplitude of the peak was 0.5 to 1 standard deviations. Of the 69 peaks observed in the Mg/Ca profile, 42 (61%) could be robustly matched and another 20 (29%) tentatively matched, leading to only 7 (10%) Mg peaks without CL match.

3.4. $\delta^{13}C$ and $\delta^{18}O$ values

$\delta^{13}C$ values of the barnacle data set span a large range from −6.8 to +2.6‰ (Fig. 7). Typical interquartile ranges

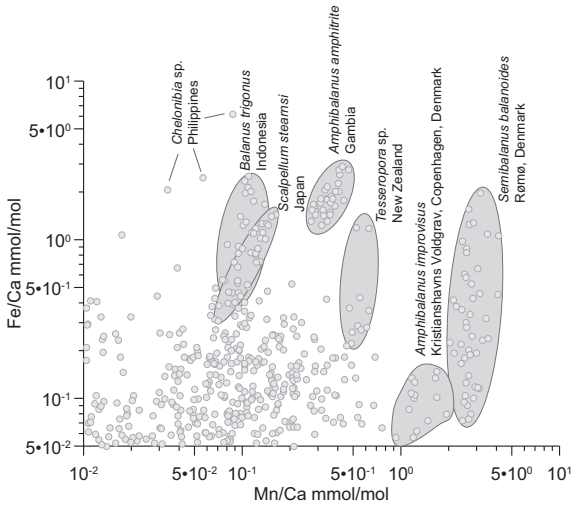

Fig. 4. Mn/Ca and Fe/Ca ratios in investigated barnacle species. Specimens for which either ratio surpasses 1 mmol/mol in multiple instances are marked. Samples with element/Ca ratios below detection limit are not shown (Mn/Ca: 299 samples, 26% of the total; Fe/Ca: 544 samples, 48% of the total).

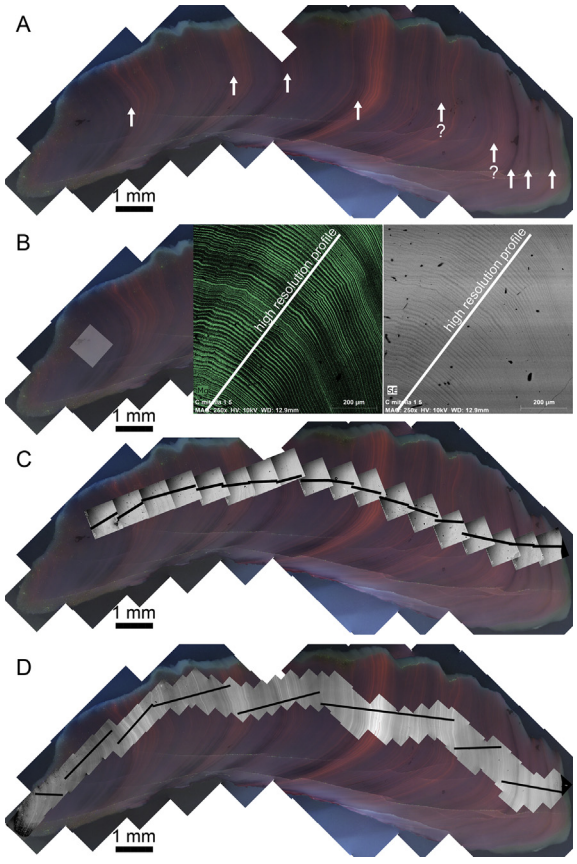

Fig. 5. CL, energy dispersive spectrometry (EDS) and backscatter electron (BE) images of carina of *C. mitella*. A: Mosaic of CL images with tentative positions of boundaries between ten zones defined by a thicker, luminescent and thinner, weakly luminescent band. These zones are interpreted to represent annual growth patterns. The growth direction is to the right. B: Same mosaic with white square indicating the position of SEM-based Mg map and SE image (to the right). C: Same mosaic with overlay of BE images and traces where Mg/Ca ratios were analysed using SEM-based EDS. Traces of the high resolution profiles are indicated as white lines on these maps. D: Same mosaic with overlay of high-resolution CL images and traces for which CL intensity was quantified.

of $\delta^{13}C$ values for the localities are 0.4‰, but at a few localities (*Lepas anserifera*, one specimen; *Solidobalanus fallax*, two specimens) a considerably larger interquartile spread of 1.5 and 3.0‰, respectively, is observed. Species with the lightest median $\delta^{13}C$ values (*Amphibalanus improvisus*, −5.8‰; *Dosima fascicularis*, −4.3‰) are from very nearshore settings in central Copenhagen and Skagen, Denmark. Amongst the barnacle orders, the Lepadiformes have a tendency to lighter $\delta^{13}C$ values (median = −1.7‰; 5 species) than scalpelliform barnacles (median = −0.5‰; 10 species) and balaniform barnacles (median = +0.4‰; 25 species).

$\delta^{18}O$ values of the entire data set range from −5.0 to +5.0‰ (Fig. 7). Typically, interquartile ranges of oxygen isotope ratios for single localities are smaller (0.2‰) than for carbon isotopes and exceed 1‰ only in a specimen of *Striatobalanus amaryllis* from the Persian Gulf. Species with

the lightest $\delta^{18}O$ values (*Amphibalanus improvisus*, 2 localities, −4.6 and −3.6‰) come from reduced salinity environments in the Baltic Sea. Other specimens with median values < −2‰ ($n = 4$) were collected in tropical localities (Singapore, −2.8‰; Singapore, −2.6‰; Gambia, −2.5‰; Hong Kong, −2.1‰). Conversely, specimens with the heaviest median values either come from high latitudes (*Balanus balanus*, +4.4‰, ~78°N; *Semibalanus balanoides*, +2.1‰, ~65°N) or deep water settings (*Metaverruca recta*, +3.7‰, Rodrigues Ridge, 2600 m; *Eochionelasmus ohtai*, +3.2‰, North Fiji Basin, 1990 m; *Neoscalpellum* sp., +3.1‰, Porcupine Seabight, 484 m).

No clear relation of $\delta^{13}C$ with $\delta^{18}O$ is apparent for the entire dataset ($r^2 = 0.06$), where only *A. improvisus* from central Copenhagen shows median values substantially lower than −2‰ in both isotopic systems. Strong correlations ($r^2 > 0.6$), however, are observed at several localities. Specimens of three of five lepadid species (*D. exoleta*, one specimen; *D. fascicularis*, one specimen; and *L. pectinata*, two specimens) show strong covariation of carbon and oxygen isotope ratios ($r^2 = 0.60, 0.64, 0.71$) with positive slopes of $\delta^{18}O = 0.3–0.4 * \delta^{13}C$ (Fig. 8). Strong covariation of these proxies are also noted in both studied representatives of *Megabalanus* ($r^2 = 0.62, 0.75$) and in one of two specimens of *Striatobalanus amaryllis* ($r^2 = 0.46, 0.72$). For both genera the slopes of these co-variations are opposite between the two specimens, however. Correlations of element proxies with isotope ratios for the entire data set are generally very weak ($r^2 < 0.15$).

4. DISCUSSION

4.1. Sr vs Mg in biogenic calcite

Since early assessments of Sr and Mg contents of biogenic aragonite and calcite (Odum, 1951; Dodd, 1967), work on mapping the chemical composition of marine calcifying species has been mostly undertaken on single species. Such studies were predominantly concerned with developing new palaeoenvironmental proxies or gaining a better understanding of the biomineralisation process (e.g., Dodd, 1965; Bourget, 1974; Freitas et al., 2006). A

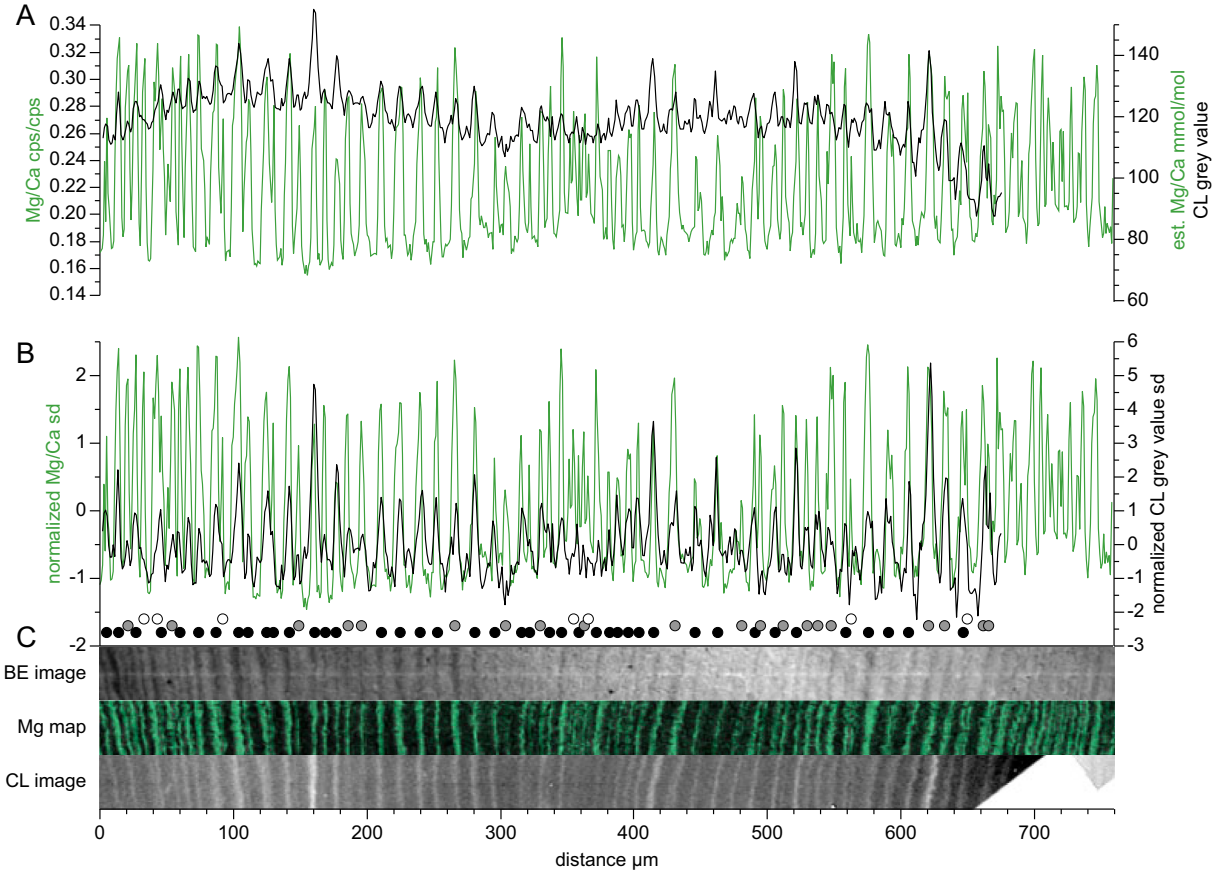

Fig. 6. High resolution Mg/Ca and CL patterns in specimen of *Capitulum mitella*. (A) Mg/Ca (green curve) and CL intensity (black curve) along a c. 750 µm long trnsect through a *C. mitella* carina. Tentative quantification of raw Mg/Ca ratios is based on an assumed average Mg/Ca ratio of 88 ± 6 mmol/mol (2 se, $n = 25$) in this species. (B) Detrended, normalized data from (A) and peak matching results for the high resolution transect. Black circles indicate a robust match, gray circles a tentative match and white circles a mismatch of the peaks in the two transects (see Section 3.3 for further information). (C) SEM-based BE image (top), Mg map (middle), as well as CL image (bottom) for this transect are shown in the bottom part of the figure. The growth direction is to the right. (For interpretation of the references to colour in this figure legend, the reader is referred to the web version of this article.)

general view is that biogenic calcite shows a broad positive correlation between Sr and Mg, and is enriched in Sr with respect to abiogenic calcite precipitates with a comparable Mg/Ca ratio (Carpenter and Lohmann, 1992). This assessment holds for the comparatively well-studied brachiopods, which cover a wide range of Mg/Ca ratios and reach maximum Sr/Ca ratios of ~3 mmol/mol in the high Mg calcite of craniid brachiopods (Fig. 9; Supplementary Table 4; see data in Brand et al., 2003).

Biogenic LMC with Sr/Ca ratios of 1 to 2 mmol/mol is ubiquitous (Fig. 9), in good agreement with precipitation-rate dependent Sr distribution coefficients of 0.07–0.24 in abiogenic calcite at typical marine pH (Tang et al., 2008; DePaolo, 2011). From these distribution coefficients Sr/Ca ratios of 0.6–2.1 mmol/mol for calcite are predicted to precipitate from modern seawater. A considerably wider range of compositions is allowed if changes in pH are permitted (Tesoriero and Pankow, 1996; DePaolo, 2011), helping to explain the partly very low Sr concentrations observed in abiogenic marine calcite (Carpenter and Lohmann, 1992). Sr/Ca ratios consistently greater than 2 mmol/mol in modern biogenic calcite are seldom observed, and a miscibility gap between $SrCO_3$ and $CaCO_3$ limits the amount of Sr that can be accommodated in the calcite crystal lattice. Even though experimental results on this miscibility gap below 350 °C and ambient pressure are missing (Carlson, 1980), the upper limit of Sr uptake has been proposed to be near Sr/Ca ratios of ca. 5 mmol/mol (Tesoriero and Pankow, 1996). Crystal lattice distortions in biogenic calcite induced by the incorporation of organic macromolecules (Pokroy et al., 2006) may allow for even higher Sr/Ca ratios in shell calcite and explain the otherwise surprisingly high Sr/Ca ratios in arthropod calcite (Fig. 9).

The Sr/Ca and Mg/Ca pattern of barnacle calcite stands in strong contrast to other biogenic, marine calcite. When incorporated into a comprehensive dataset of marine shell calcite the observed signatures of arthropod Sr/Ca are distinctly higher than other biogenic calcite at comparable Mg/Ca ratios (see also Carpenter and Lohmann, 1992). Despite the nearly exclusive secretion of LMC, barnacle calcite shows very high Sr concentrations indicating Sr distribution coefficients of 0.3–0.7. High Sr/Ca ratios are not uncommon for arthropods (e.g., decapods, Gibbs and Bryan, 1972), but barnacles differ from decapods by almost exclusively forming LMC

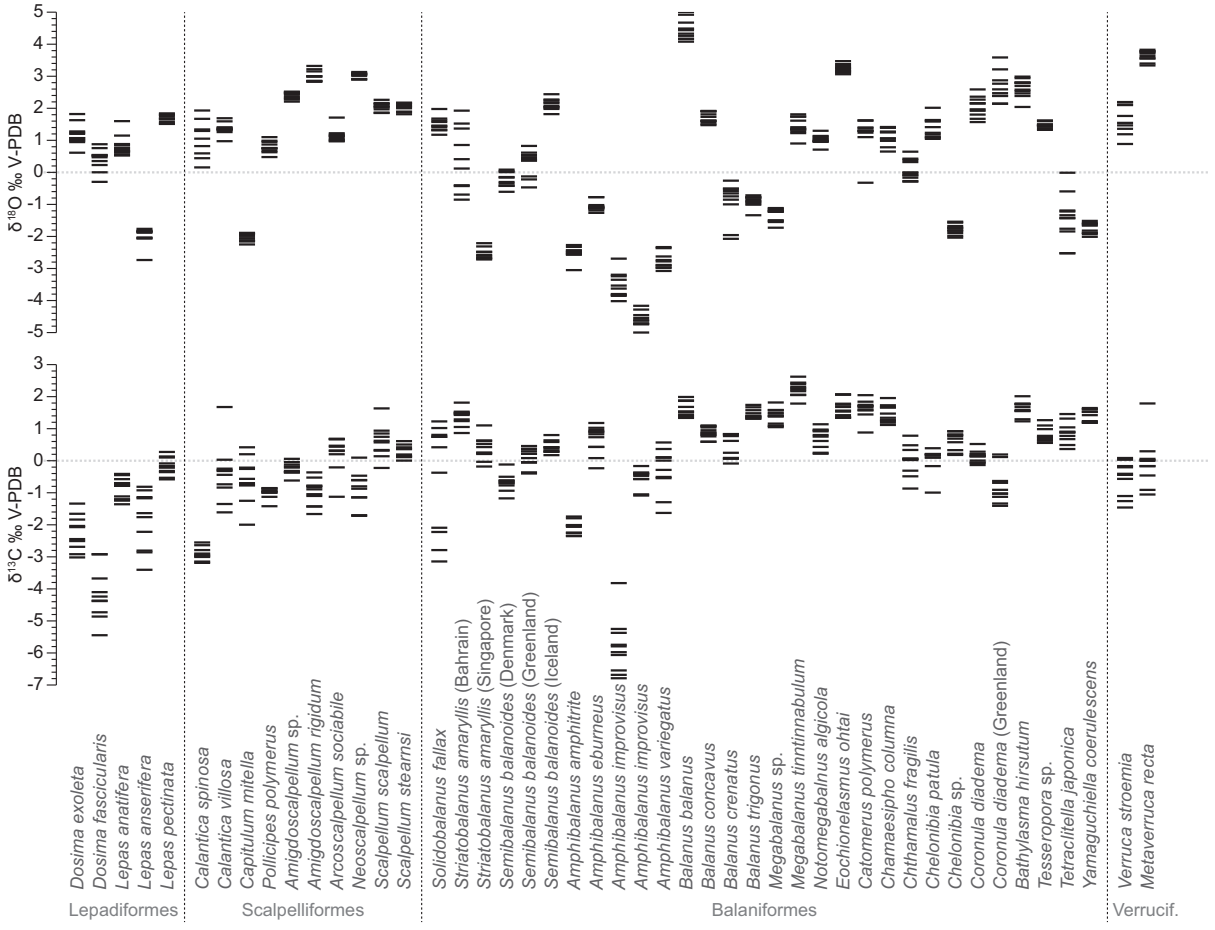

Fig. 7. Oxygen and carbon isotope ratios measured for the barnacles from 47 localities. Samples from fresh water-influenced areas and warm water habitats generally show low $\delta^{18}O$ values and samples from deep water and high latitude environments high $\delta^{18}O$ values.

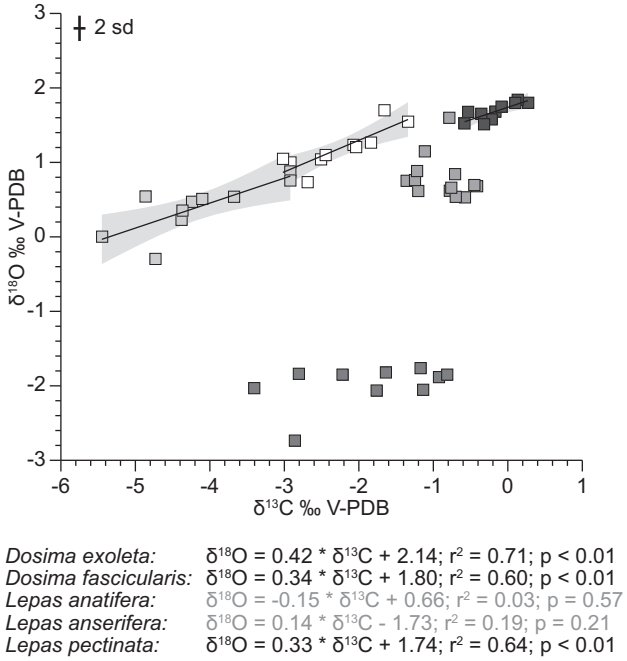

Fig. 8. Cross plot of oxygen and carbon isotope ratios in calcite of Lepadiformes. Strong positive correlations are observed in representatives of three of five investigated species indicating isotopic disequilibrium of variable magnitude during shell formation.

rather than HMC. Sr and Mg signatures similar to cirripedes are observed for marine ostracodes (Fig. 9; Dwyer et al., 2002). Very few species of marine ostracodes have, to date, been studied for their shell geochemistry, so the potential range of composition in this group is not yet well constrained. It has been hypothesized that the calcite secreted by crustaceans is particularly Sr-rich because of very high shell secretion rates in this group of animals (Carpenter and Lohmann, 1992). The result would be an arthropod-specific covariation of Sr and Mg concentrations at elevated Sr concentrations. However, organisms which secrete shell calcite much faster than barnacles have comparatively low Sr/Ca ratios. Oyster specimens studied by Ullmann et al. (2013b) for example reached heights of 17–19 cm in four years but only have average Sr/Ca ratios of 0.81 mmol/mol. Bivalves in general, which on average exhibit much faster metabolic rates than brachiopods (Payne et al., 2014) and secrete shell calcite more rapidly, do not show any tendency to higher Sr/Ca ratios than brachiopods (Fig. 9). Furthermore, it has been shown experimentally (Gabitov et al., 2014) and observed in biogenic calcite (Ullmann and Pogge von Strandmann, 2017) that secretion rate-related effects on element uptake in biogenic calcite should lead to a negative correlation of Sr/Ca with Mg/Ca ratios. This negative correlation, however, is not observed as an overarching control on crustacean calcite composition (Fig. 9). These factors taken together rather suggest that shell secretion rate is not the primary driver for the Sr enrichment in cirripedes.

Even though the causes, utility, and mechanisms of Sr enrichment in biogenic calcite remain poorly understood, the empirically constrained species-specific elemental fingerprints of biogenic calcite can nevertheless be utilized. In particular, the various specific combinations of Sr/Ca and Mg/Ca ratios in biogenic calcite may be highly beneficial to trace the chemical composition of seawater through time. Previously, a constant Sr distribution coefficient of 0.41 equating to a barnacle Sr/Ca ratio of 3.8 mmol/mol was proposed for intertidal barnacles on the basis of data from four species (Bourget, 1974; Smith et al., 1988). The more comprehensive dataset assembled here for four cirripede orders suggests an average of 4.2 ± 0.2 mmol/mol (2 se, $n = 47$) which nearly coincides with the earlier estimate. When applied to single species, such an assumption of constant Sr/Ca is clearly an oversimplification (Fig. 9) and some minor, but significant differences in Sr/Ca and Mg/Ca have been identified between scalpelliform barnacles from various localities (*Pollicipes pollicipes*, Albuquerque et al., 2016). Using taxonomically identified barnacle calcite, however, could still be valuable for seawater Sr/Ca reconstruction. Nevertheless, clear concerns for robust seawater element/Ca reconstruction include: complicated response of biomineral element/Ca to seawater element/Ca ratios (Segev and Erez, 2006), temperature (Dodd, 1965; Cléroux et al., 2008), growth rate (Gillikin et al., 2005; Ullmann and Pogge von Strandmann, 2017), and diagenesis (Brand and Veizer, 1980; Al-Aasm and Veizer, 1986). If a variety of marine calcites shows consistent offsets and trends through time (e.g., Ullmann et al., 2013c), confidence in the reconstruction of seawater composition, however, can be substantially improved. To this end, barnacles can become a useful additional archive because of the Sr-enriched LMC of their shell material.

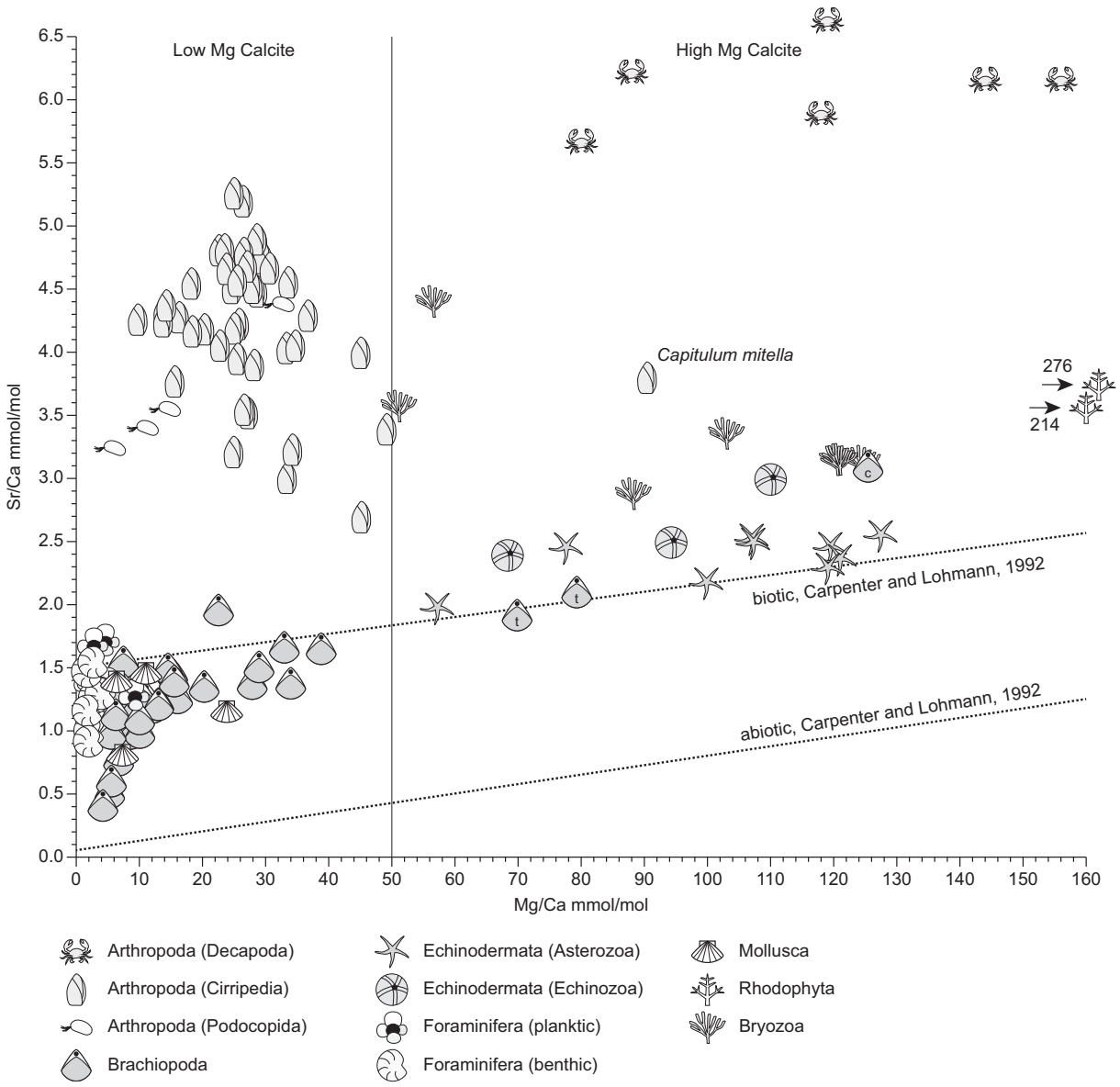

Fig. 9. Average Mg/Ca and Sr/Ca ratios for barnacle species analysed here as well as Sr/Ca and Mg/Ca ratio averages for other calcite secreting species taken from the literature (Pilkey & Hower, 1960; Schopf & Manheim, 1967; Gibbs & Bryan, 1972; Delaney et al., 1985; Carpenter & Lohmann, 1992; Cronin et al., 1996; Klein et al., 1996; Rathburn and De Dekker, 1997; Almeida et al., 1998; De Dekker et al., 1999; Brand et al., 2003; Vann et al., 2004; Freitas et al., 2005,2006; Hermans et al., 2010; Iglikowska et al., 2018b; Supplementary Table 4). Brachiopods marked with "t" belong to the Thecideida and the species marked with "c" is a craniid brachiopod. Tentative trends of biotic and abiotic calcite from Carpenter and Lohmann (1992) are also shown.

4.2. Mg/Ca heterogeneity in shell plates of barnacles

4.2.1. Mg/Ca variability in single specimens

For 12 species (15 sites; Supplementary Table 5) of balaniform cirripedes for which scuta, terga, and wall plates were available for analysis, a significant enrichment of Mg in scuta and terga over Mg/Ca in the wall plates is observed (Fig. 10). On average, Mg/Ca ratios of the scuta are $32 \pm 6\%$ and Mg/Ca ratios of terga $41 \pm 8\%$ (2 se) higher than Mg/Ca ratios in the wall plates and most species show slightly higher Mg/Ca ratios in terga than in scuta. A ca 60% enrichment of Mg in scuta and terga (not distinguished) with respect to the wall plates has also been observed for the sessile barnacle *Balanus balanus* (Iglikowska et al., 2018a). In nine species of scalpelliform barnacles, no such enrichment of Mg is observed (Fig. 10, Supplementary Table 5). Here, scuta have $97 \pm 6\%$ and terga $98 \pm 8\%$ (2 se) of the Mg content of other plates. Also in two species of *Lepas* (Lepadiformes) for which various plates could be measured, Mg/Ca ratios of scuta and terga coincide with those of other plates within uncertainty. For the two verruciform species studied here, neither scuta nor terga were available, so that their Mg incorporation behaviour could not be addressed. The strong Mg enrichment

in the scuta and terga of Balaniformes does explain the observation of higher Mg variability in their shell material as compared to other barnacle orders (Section 3.1).

Mg-enriched parts of biogenic shells controlled by functional morphology are not restricted to the Balaniformes but are known from echinoderms (Davies et al., 1972; Busenberg and Plummer, 1989; Ries, 2011; Iglikowska et al., 2018b), brachiopods (Pérez-Huerta et al., 2008; Ullmann et al., 2017) and bivalves (Freitas et al., 2009). The consistency of the observed Mg enrichment in the scuta and terga of balaniform barnacles, however, is striking. The homology of shell plates in the Thoracica (encompassing all sessile and stalked barnacles) has been proposed (Pérez-Losada et al., 2008). It is intriguing in this context that a shared phylogenetic blueprint of the various shell plates does not seem to be mirrored in similar element concentration patterns across all barnacle species. A particular form of bioengineered calcite geochemistry for movable shell plates as opposed to the fixed wall plates in Balaniformes is an intriguing observation which warrants further study.

4.2.2. Mg/Ca as a temperature proxy in barnacles?

A direct relationship between temperature and Mg concentration in barnacle calcite has been proposed on the basis of a small set of specimens with mostly unknown taxonomic designation (Chave, 1954). A monospecific dataset of *Tetraclita serrata* from South Africa broadly confirmed such a relationship but pointed to a large uncertainty of any temperature calibration of barnacle Mg/Ca (Smith et al., 1988). Additionally, a strong Mg gradient within single shell plates was observed using electron probe microanalysis which was tentatively related to dissolution-precipitation reactions in the intertidal zone (Smith et al., 1988). A possible temperature effect on Mg uptake in barnacle calcite was also suggested for barnacles from the coast of Wales and Irish Sea (Bourget, 1974), but growth rate was deemed to be the dominant forcing on shell element/Ca ratios in that study.

In the present dataset covering a wide range of species the lowest Mg/Ca ratios from 4–12 mmol/mol occur in whale barnacles (*Coronula diadema*) collected in Greenland and the highest ratios of 65–105 mmol/mol in *C. mitella* from Hong Kong. These data are compatible with a temperature control on Mg/Ca. Phylogeny, however, seemingly exerts the prevalent control on skeletal Mg/Ca ratios: comparatively high Mg/Ca ratios are also observed in the cold water specimen of *Metaverruca recta* from ca. 2.6 km depth (31–65 mmol/mol) and lower ratios of 18 to 44 mmol/mol in *Amphibalanus variegatus* from the warm waters of Singapore.

Nevertheless, the derivation of species-specific Mg/Ca thermometers might be possible: Specimens of *Semibalanus balanoides* from Greenland, Iceland and Denmark exhibit different Mg/Ca ratios across a gradient of annual average temperatures from ca. 2 °C (Greenland) to 10 °C (Denmark) (WOD13, Boyer et al., 2013). The Danish specimens experienced the highest ambient temperatures and, as expected, show the highest Mg/Ca ratios in wall plates, scuta and terga (Fig. 11). The Mg/Ca ratios of the Greenland specimen that secreted its shell in the coldest water, however, are not consistently the lowest. The tight correlation of Mg/Ca data with temperature in the terga of *S. bal-*

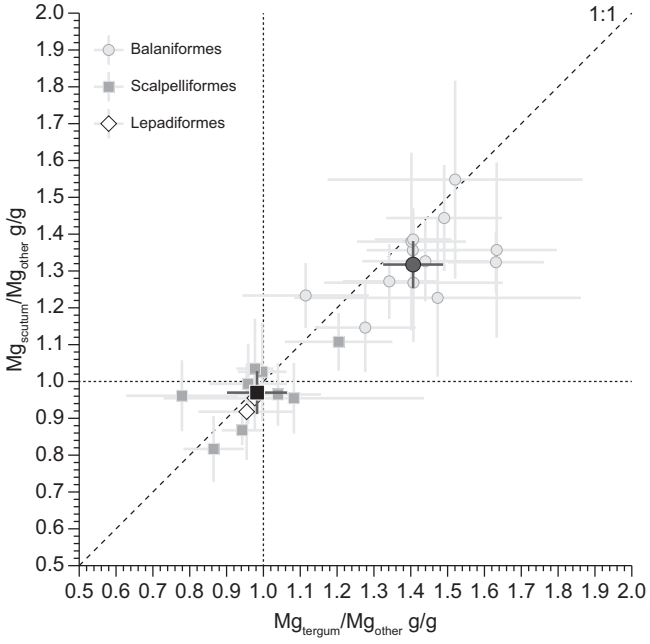

Fig. 10. Enrichment factors of Mg in scuta and terga of the investigated barnacle species (see also Supplementary Table 5). Small symbols represent individual species and larger symbols the averages for Balaniformes and Scalpelliformes. Mg in scuta and terga of balaniform barnacles is significantly enriched with respect to Mg in wall plates. For individual species, error bars are 2 se (standard error) of the analytical results. For the pooled data for Balaniformes and Scalpelliformes, error bars indicate 2 se of the species averages. No data for verruciform barnacles is available.

anoides is likely caused by a sampling effect. The terga of this species are relatively small, so that material extracted from them are more likely to constitute representative samples than material taken from the larger scuta and wall plates.

An increase of Mg/Ca can also be read from data for *Striatobalanus amaryllis* from the Persian Gulf (ca. 25 °C) and Singapore (ca. 29 °C) (WOD13, Boyer et al., 2013), where *S. amaryllis* from Singapore shows on average 5 mmol/mol higher Mg/Ca ratios. These data suggest that a control of Mg/Ca in barnacles linked to changes in temperature may exist and could lead to the development of species-specific Mg/Ca thermometers (see also Bojar et al., 2018). The barnacle calcite, however, generally exhibits large heterogeneity in Mg/Ca ratios even in environments where seasonal temperature variability is much reduced. This heterogeneity implies that such a thermometer would only be useful in environments with reduced and variable salinity, where the oxygen isotope thermometer could not be employed or would be less precise (see also Smith et al., 1988).

4.3. Mn/Ca and Fe/Ca in barnacle calcite

Mn/Ca and Fe/Ca ratios in biogenic calcite are most commonly taken to address the preservation state of fossil materials. Both, Mn and Fe concentrations are typically very low in marine environments (Milne et al., 2010; Biller and Bruland, 2012), such that substantial enrichments in these elements in fossil shell materials are good indicators of diagenetic overprint (see Ullmann and Korte, 2015 for a review). In proximal shelf areas, however, Mn can be made available for biomineralisation through biogeochemical pathways (Vander Putten et al., 2000) and seasonal temperature and sediment redox variation (Morris, 1974; Freitas et al., 2006) or be a sign of disease (Almeida et al., 1998).

In barnacles, dominant controls on shell Mn/Ca ratios, however, appear to be ambient water Mn concentrations (Gordon et al., 1970, see also Hockett et al., 1997) and possibly salinity (Pilkey and Harriss, 1966). Continental or anthropogenic Mn sources as in the case of Chesapeake Bay (Gordon et al., 1970) may thus leave a strong imprint on barnacle calcite, particularly in species living close to such sources in intertidal environments. Also, barnacles appear to have a much stronger affinity for incorporation of Mn into their shells than other sessile calcifiers like oysters (Pilkey and Harriss, 1966), possibly related to growth rate or organic matter associated with shell calcite (Bourget, 1974). Similar controls can be envisioned for the incorporation of Fe into barnacle calcite.

The absolute levels of Mn and Fe in barnacle shell material may thus be first and foremost an indication of habitat and even Mn/Ca and Fe/Ca ratios > 4 mmol/mol (Supplementary Table 1; Fig. 4; Pilkey and Harriss, 1966) can be reached in primary calcite. When employing Mn and Fe as preservation markers for fossil barnacles, it is therefore of importance to check for other known elemental and isotopic co-variations produced by diagenesis, as well as assessing the spatial distribution of Mn and Fe.

4.4. Tidal control on element distribution in *Capitulum mitella*?

Growth functions of *C. mitella* (Nakamura and Tanaka, 1995) and decreasing thicknesses of the ten broader zones delineated by CL in the investigated carina of this species (Figs. 5 and 6; Table 2) suggest that these are the expression of annual cycles of shell secretion. The exact sample locality and data for the specimen of *C. mitella* is unknown – it was sampled in the intertidal zone in Hong Kong in the early 20th century (Table 1). This lack of exact provenance data and the complicated tidal regime in the Pearl River estuary (Mao et al., 2004) make exact reconstructions of

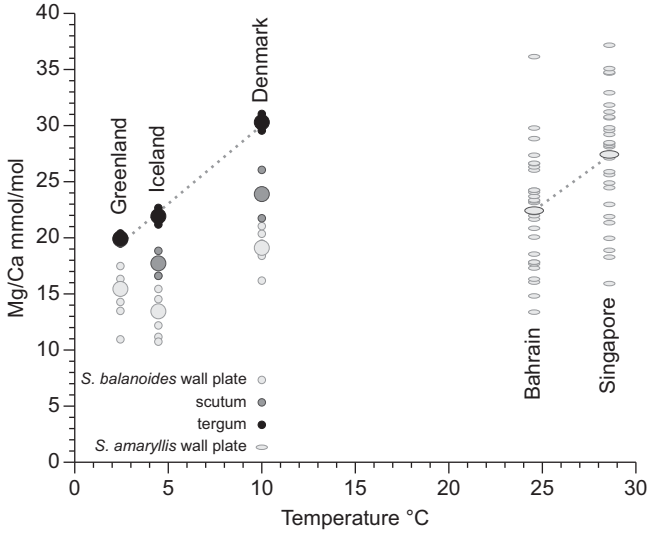

Fig. 11. Mg/Ca ratios in *Semibalanus balanoides* and *Striatobalanus amaryllis* from various localities. A broadly positive correlation of Mg/Ca ratios with temperature is observed for both species. Large symbols designate average value for shell plate type for each sample location.

environmental parameters at the life time of the barnacle impossible. Increased discharge of Mn in the Pearl River in the spring, however, could explain the more prominent luminescent bands at the beginning of an annual zone which are then followed by bands that are overall less luminescent. Alternatively, Mn enrichments could be associated with increased amounts of intracrystalline organic matter (Bourget, 1974), which may occur as part of the animal's seasonal growth cycle.

Durations of 1.3–1.8 days have been proposed for the formation of growth ridges on plates of *Balanus amphitrite* (Clare et al., 1994), features which are controlled by the molting cycle (Chave, 1984). For internal banding, however, a strong control on immersion time and the tidal cycle have been observed in *Semibalanus balanoides* (Bourget and Crisp, 1975) and *Elminius modestus* (Crisp and Richardson, 1975). The average thickness of the thin luminescent bands in *C. mitella* is similar to these examples and suggests that the bands may be related to the tidal cycle.

Distances between intensity peaks are usually 5–15 μm in the juvenile and early adult part in *C. mitella*, where the broader, possibly annual zones are 2–3 mm thick (Fig. 5; Table 2; Supplementary Tables 2 and 3). Regions with indistinct bands, complicated peak shapes and high-frequency oscillations preclude an exact assessment of the number of bands within a single zone. The average distance between CL peaks, however, makes it possible that the number of bundles of luminescent and non-luminescent calcite within a zone is controlled by daily or tidal cycles. Considering the intertidal habitat of *C. mitella* it is probable that the tidal cycle exerts a prominent control on the barnacle metabolism, even though this hypothesis requires further testing. If tides are indeed the main drivers of growth bands in *C. mitella*, the less luminescent bands may be formed during immersion at high tides, whereas more Mn-enriched calcite is formed when restricted tidal pools develop at low tides and barnacles close their shell plates until immersion re-occurs (Craven et al., 2008).

The extraordinary control on both Mn and Mg incorporation, the comparative ease with which both these parameters can be measured in *C. mitella*, as well as the comparative longevity of *C. mitella* could make this species a very important archive for reconstructing continental runoff and tidal dynamics in recent and fossil settings. Collection and study of modern *C. mitella* from well constrained sites will be important to verify these hypotheses.

4.5. C and O isotopes in barnacle calcite

4.5.1. Oxygen isotope thermometry

4.5.1.1. ^{18}O enrichment in barnacles. A precise, barnacle-specific oxygen isotope thermometer is available over a wide range of temperatures (c. −2 to +26 °C, Killingley and Newman, 1982). This thermometer is based on oxygen isotope ratios in the calcite shells of a variety of barnacle species and predicts considerably higher temperatures for a given shell $\delta^{18}O$ value than other common oxygen isotope thermometers. For example, the offset from the Epstein et al. (1953) equation is between 2.7 °C at the low end and 5.7 °C at the high end of the calibrated temperature range, suggesting that barnacles secrete their shells with increased oxygen isotope fractionation factor, i.e. preferentially incorporating the heavy oxygen isotopes. A series of studies on barnacle calcite have indirectly or directly commented on this surprising finding, which has been related to poorly understood disequilibrium incorporation of oxygen isotopes into shell calcite (McConnaughey, 1989a):

Table 2
Positions of boundaries between zones delineated by cathodoluminescence in carina of *Capitulum mitella*.

Subdivision no	Position (mm)	Thickness (mm)
1	2.69	>2.69
2	5.73	3.04
3	7.17	1.44
4	9.24	2.07
5	11.20	1.96
6	12.58	1.38
7	13.16	0.58
8	13.48	0.32
9	14.01	0.53
Edge	14.33	0.32

At one extreme, ^{18}O enrichment even beyond the Killingley and Newman (1982) barnacle thermometer has been proposed for the green sea turtle barnacle *Platylepas* by comparison of predicted and observed $\delta^{18}O$ values in barnacle shells on turtles in the Palmyra Atoll National Wildlife Refuge (Detjen et al., 2015). At the other extreme, the Killingley and Newman (1982) thermometer has been rejected for the cold-water barnacle *Bathylasma corolliforme* from the McMurdo Ice Shelf, Antarctica (Burgess et al., 2010). Burgess et al. (2010) found the same $\delta^{18}O$ values as Killingley and Newman (1982) who studied the same species at a site within a few kilometres and the same oceanographic conditions. However, in the absence of seawater oxygen isotope data at the time, Killingley and Newman (1982) argued that a +1.0‰ offset of *B. corolliforme* from the gastropod *Limatula* at the same locality confirmed their thermometer. Conversely, Burgess et al., (2010), relying on measurements of Ross Sea water and a proposed general model of water circulation at the Ice Shelf (Jacobs et al., 1985), argued for isotopically comparatively heavy sub-ice seawater. These seawater isotope ratios in turn led to estimated barnacle oxygen isotope fractionation factors in close agreement with mollusc, foraminifer and abiogenic calcite (Burgess et al., 2010).

Most commonly, however, it is stated that barnacle calcite is comparatively rich in ^{18}O (Newman and Killingley, 1985; Smith et al., 1988; Craven et al., 2008), particularly when compared against mollusc carbonate from the same sites (Killingley and Newman, 1982; Brand et al., 1987). It thus appears that barnacles have a tendency to secrete comparatively ^{18}O-rich shell calcite.

Somewhat uncertain provenance, water composition and annual temperature ranges at the sites of collection for the present dataset preclude a meaningful discussion of minor deviations of calcite-water oxygen isotope fractionation factors. No bias towards heavy oxygen isotope ratios, however, is required to explain observed values in

deep marine barnacle for which strong fresh water input as a potential bias of shell $\delta^{18}O$ can be excluded: Using a deep sea water $\delta^{18}O$ estimate of -0.1‰ SMOW (Bigg and Rohling, 2000) and the Killingley and Newman (1982) isotope thermometer for *Metaverruca recta*, a $\delta^{18}O$ value of +4.9‰ would be expected from temperatures of +2 °C at the approximate sample position (WOD13, Boyer et al., 2013). A much less positive range of values of +3.3 to +3.8‰ is observed, however, which is much more compatible with commonly employed thermometers of Epstein et al. (1953) as well as Anderson and Arthur (1983). The same conclusions can be drawn for *Eochionelasmus ohtai* from the North Fiji Trench, for which an expected $\delta^{18}O$ value of +4.9‰ stands in contrast to observed values between +3.1 to +3.5‰.

Despite the uncertain absolute oxygen isotope fractionation factor for barnacles, a strong temperature dependence on $\delta^{18}O$ in their calcite is evident (e.g., Killingley and Newman, 1982). Reconstructions of relative temperature changes from barnacle shells are therefore possible where other complicating factors such as variable $\delta^{18}O$ of ambient water are negligible.

4.5.1.2. Mg-effect on oxygen isotope fractionation factor. A systematic increase of oxygen isotope fractionation factors in calcite with increasing Mg substitution of the Ca site has been found (Tarutani et al., 1969; Jiménez-López et al., 2004). Proposed magnitudes of these effects are +0.06‰ per mol% $MgCO_3$ (Tarutani et al., 1969) or +0.17 ±0.02‰ (Jiménez-López et al., 2004). The latter was adopted for an empirical calibration of brachiopod data (Brand et al., 2013). The median Mg/Ca ratio of 25 mmol/mol (interquartile range of 19–31 mmol/mol) for the entire barnacle dataset equates to approximately 2.5 (~1.9–3.1) mol% $MgCO_3$ (discounting a small offset due to the presence of other impurities such as $SrCO_3$ etc.). Adopting the recent estimate of the Mg effect on oxygen isotope fractionation, barnacle calcite may thus be enriched in ^{18}O by 0.43 (0.32–0.53) ‰ with respect to pure calcite. Calcite oxygen isotope thermometers are usually calibrated on materials with low Mg/Ca ratios such as pure calcite (O'Neil et al., 1969; Kim and O'Neil, 1997) or foraminifera (Shackleton, 1974; Erez and Luz, 1982). The generally higher Mg/Ca ratios of barnacles may therefore account for some of the proposed 1.3‰ offset (Killingley and Newman, 1982), but the magnitude of the correction is insufficient to reconcile the available oxygen isotope thermometers. Other effects such as pH of fluids at the site of shell secretion (e.g., Dietzel et al., 2009), or biological control on the oxygen isotope equilibration time and carbonate precipitation mechanism (Taubner et al., 2012 and references therein) would have to be invoked to explain remaining discrepancies in the oxygen isotope thermometers.

4.5.2. Vital effects on C and O isotope ratios in barnacles

Reports of carbon isotope ratios in barnacles have so far been restricted to balaniform barnacles and values have mostly been interpreted to be compatible with equilibrium shell formation (Brand et al., 1987). Minor deviations (<1‰) towards more negative values have been related to reduced immersion time and to increased aperture diameter (Craven et al., 2008). Large contributions of metabolized carbon to tissues and shell of *Balanus* spp. have previously been reported (Tanaka et al., 1986). Amongst the taxa studied by Tanaka et al. (1986), the barnacle specimen, however, showed the lowest calculated contribution of metabolized organic carbon whose overall contribution was later revised towards much lower values (McConnaughey et al., 1997). While $\delta^{13}C$ values in barnacle calcite are generally somewhat lower than expected from local DIC composition (Fig. 7; Emrich et al., 1970; Tagliabue and Bopp, 2008), these deviations are not major, further supporting the small contribution of metabolized carbon to the shell calcite.

Balaniform, verruciform and scalpelliform barnacles studied here show no clear evidence of kinetic isotope effects *sensu* McConnaughey (1989a,1998b). Three of five lepadid species, however, exhibit strong positive covariation of $\delta^{13}C$ values with $\delta^{18}O$ values and ^{13}C and ^{18}O depleted calcite with the typically observed stronger depletion of the heavy carbon isotopes (Wefer and Berger, 1991; Carpenter and Lohmann, 1995). *D. fascicularis* specimens which showed the strongest depletion of ^{13}C amongst the lepadids were sampled as part of a barnacle mass occurrence that left numerous individuals stranded on beaches in Northern Jutland (Denmark). Kinetic isotope fractionation induced by accelerated growth rate leading to a depletion of the heavy isotopes in these specimens would thus not be surprising.

5. CONCLUSIONS

The present dataset constitutes the first large survey of barnacle shell geochemistry, confirming and refining known patterns of element/Ca as well as C and O isotope ratios in barnacle calcite and pointing to their potential use as proxies for palaeoenvironmental conditions.

Barnacles generally secrete low-Mg-calcite with very high Sr/Ca ratios, but also some cases of high-Mg-calcite, in particular *Capitulum mitella*, are observed where Sr/Ca ratios are equally high. The Mg-enriched nature of *C. mitella*, intertidal habitat, and clear banding pattern in the shell make it a potential archive for reconstructing the tides, seasonality and terrestrial element fluxes into shallow marine environments from fossil representatives of this species.

A possible temperature control on Mg/Ca ratios in barnacles is confirmed, but heterogeneity of shell material and species-specific Mg distribution coefficients complicate the derivation of robust Mg thermometers for barnacles. Barnacle Mg thermometry may nevertheless be useful in estuarine and near-shore environments, where $\delta^{18}O$ values of ambient water may be highly variable.

Barnacles from very near-shore localities and those attached to manmade structures can incorporate very high amounts of Mn and Fe into their shell calcite (Mn/Ca and Fe/Ca > 4 mmol/mol) which has to be considered when studying fossil barnacles.

Balaniform barnacles exhibit a strong Mg enrichment in their scuta and terga over other shell plates (32 ± 6 and

41 ± 8‰), a geochemical pattern which is not observed in other barnacle orders.

No clear indication for strong disequilibrium isotope incorporation has been detected in balaniform, verruciform and scalpelliform barnacles permitting their use for reconstructions of palaeotemperatures, or at least relative temperature changes. The majority of lepadiform barnacles, however, appear to preferentially incorporate the light carbon and oxygen isotopes into their shell calcite.

ACKNOWLEDGEMENTS

The authors thank three anonymous reviewers for their insightful and constructive comments that helped to substantially improve the clarity and quality of the manuscript. The authors acknowledge the Natural History Museum of Denmark (Zoological Museum) for permitting destructive sampling of archived specimens (numbers 2, 4, 17-27, 29, 30, 32, 33, 37, 41, 45) and Jens Høeg for help during work in the archives of the Zoological Museum. CVU acknowledges funding from the Leopoldina – German National Academy of Sciences (grant no. LPDS 2014-08) and CVU and SPH acknowledge funding from the Natural Environment Research Council (NERC) (grant no. NE/N018508/1). Many thanks are due to Joe Pickles for help with FEG-SEM analyses and to Steve Pendray (both University of Exeter) for barnacle thin section preparation and Bo Petersen (University of Copenhagen) for assistance with C and O isotope analysis.

APPENDIX A. SUPPLEMENTARY DATA

Supplementary data associated with this article can be found, in the online version, at https://doi.org/10.1016/j.gca.2018.09.010 and further information requested from the corresponding author.

REFERENCES

Al-Aasm I. S. and Veizer J. (1986) Diagenetic stabilization of aragonite and low-Mg calcite, I. Trace elements in rudists. *J. Sediment. Petrol.* **56**(1), 138–152.

Albuquerque R., Queiroga H., Swearer S. E., Calado R. and Leandro S. M. (2016) Harvest locations of goose barnacles can be successfully discriminated using trace elemental signatures. *Sci. Rep.* **6**, 27787. https://doi.org/10.1038/srep27787.

Almeida M. J., Machado J., Moura G., Azevedo M. and Coimbra J. (1998) Temporal and local variations in biochemical composition of *Crassostrea gigas* shells. *J. Sea Res.* **40**, 233–249.

Anderson T. F. and Arthur M. A. (1983) Stable isotopes of oxygen and carbon and their application to sedimentologic and palaeoenvironmental problems. *Soc. Econ. Paleontol. Mineral. Short Course* **10**, I.1-I-151.

Bigg G. R. and Rohling E. J. (2000) An oxygen isotope data set for marine waters. *J. Geophys. Res.* **105**, 8527–8535.

Biller D. V. and Bruland K. W. (2012) Analysis of Mn, Fe, Co, Ni, Cu, Zn, Cd, and Pb in seawater using the Nobias-chelate PA1 resin and magnetic sector inductively coupled plasma mass spectrometry (ICP-MS). *Mar. Chem.* **130–131**, 12–20. https://doi.org/10.1016/j.marchem.2011.12.001.

Bourget E. (1974) Environmental and structural control of trace elements in barnacle shells. *Mar. Biol.* **28**, 27–36.

Bourget E. (1987) Barnacle shells: composition, structure and growth. *Barnacle Biol.* **5**, 267–285.

Bourget E. and Crisp D. J. (1975) An analysis of the growth bands and ridges of barnacle shell plates. *J. Marine Biol. Assoc. UK* **55** (2), 439–461.

Bojar A.-V., Lécuyer C., Bojar H.-P., Fourel F. and Vasile S. (2018) Ecophysiology of the hydrothermal vent snail *Ifremeria nautilei* and barnacle *Eochionelasmus ohtai manusensis*, Manus Basin, Papua New Guinea: Insights from shell mineralogy and stable isotope geochemistry. *Deep-Sea Res. Part I* **133**, 49–58. https://doi.org/10.1016/j.dsr.2018.02.002.

Boyer T. P., Antonov J. I., Baranova O. K., Coleman C., Garcia H. E., Grodsky A., Johnson D. R., O'Brien T. D., Paver C. R., Locarnini R. A., Mishonov A. V., Reagan J. R., Seidov D., Smolyar I. V. and Zweng M. M. (2013) World Ocean Database 2013. In: NOAA Atlas NESDIS (eds. S. Levitus, A. Mishonov Tech), vol. 72, 209p.

Brand U. and Veizer J. (1980) Chemical diagenesis of a multicomponent carbonate system -1: trace elements. *J. Sediment. Petrol.* **50**(4), 1219–1236.

Brand U., Morrison J. O., Brand N. and Brand E. (1987) Isotopic variation in the shells of recent marine invertebrates from the Canadian Pacific Coast. *Chem. Geol.* **65**, 137–145.

Brand U., Logan A., Hiller N. and Richardson J. (2003) Geochemistry of modern brachiopods: applications and implications for oceanography and paleoceanography. *Chem. Geol.* **198**, 305–334. https://doi.org/10.1016/S0009-2541(03)00032-9.

Brand U., Azmy K., Bitner M. A., Logan A., Zuschin M., Came R. and Ruggiero E. (2013) Oxygen isotopes and $MgCO_3$ in brachiopod calcite and a new paleotemperature equation. *Chem. Geol.* **359**, 23–31. https://doi.org/10.1016/j.chemgeo.2013.09.014.

Briggs D. E. G., Sutton M. D., Siveter D. J. and Siveter D. J. (2005) Metamorphosis in a Silurian barnacle. *Proc. Roy. Soc. B* **272**, 2365–2369.

Burgess S. N., Henderson G. M. and Hall B. L. (2010) Reconstructing Holocene conditions under the McMurdo Ice Shelf using Antarctic barnacle shells. *Earth Planet. Sci. Lett.* **298**, 385–393. https://doi.org/10.1016/j.epsl.2010.08.015.

Busenberg E. and Plummer L. N. (1989) Thermodynamics of magnesian calcite solid-solutions at 25 °C and 1 atm total pressure. *Geochim. Cosmochim. Acta* **53**, 1189–1208.

Carlson W. D. (1980) The calcite-aragonite equilibrium: effects of Sr substitution and anion orientational disorder. *Am. Mineral.* **65**, 1252–1262.

Carpenter S. J. and Lohmann K. C. (1992) Sr/Mg ratios of modern marine calcite: empirical indicators of ocean chemistry and precipitation rate. *Geochim. Cosmochim. Acta* **56**, 1837–1849.

Carpenter S. J. and Lohmann K. C. (1995) $\delta^{18}O$ and $\delta^{13}C$ vales of modern brachiopod shells. *Geochim. Cosmochim. Acta* **59**(18), 3749–3764.

Chave K. E. (1954) Aspects of the biogeochemistry of magnesium 1. Calcareous marine organisms. *J. Geol.* **62**(3), 266–283.

Chave K. E. (1984) Physics and chemistry of biomineralization. *Annu. Rev. Earth Planet. Sci.* **12**, 293–305.

Christie A. O. and Dalley R. (1987) Barnacle fouling and its prevention. *Barnacle Biol.*, 419–433.

Clare A. S., Ward S. C., Rittschof D. and Wilbur K. M. (1994) Growth increments of the barnacle *Balanus amphitrite* Darwin (Cirripedia). *J. Crustac. Biol.* **14**(1), 27–35.

Cléroux C., Cortijo E., Anand P., Labeyrie L., Bassinot F., Caillon N. and Duplessy J. C. (2008) Mg/Ca and Sr/Ca ratios in planktonic foraminifera: Proxies for upper water column temperature reconstruction. *Paleoceanography* **23**. https://doi.org/10.1029/2007PA001505, PA3214.

Craven K. F., Bird M. I., Austin W. E. N. and Wynn J. (2008) Isotopic variability in the intertidal acorn barnacle *Semibalanus balanoides*: a potentially novel sea-level proxy indicator. *Geol.*

Soc. London Special Publ. **303**, 173–185. https://doi.org/10.1144/SP303.12.

Crisp D. J. and Richardson C. A. (1975) Tidally-produced internal bands in the shell of *Elminius modestus*. *Mar. Biol.* **33**, 155–160.

Cronin T. M., Dwyer G. S., Baker P. A., Rodriguez-Lazaro J. and Briggs, Jr., W. M. (1996) Deep-sea ostracode shell chemistry (Mg: Ca ratios) and Late Quaternary Arctic Ocean history. *Geol. Soc. Spec. Pub.* **111**, 117–134.

Darwin C. (1851) *A Monograph on the Fossil Lepadidae, or, Pedunculated Cirripedes of Great Britain*. Palaeontographical Society.

Darwin C. (1854) *A Monograph on the Sub-class Cirripedia*. The Ray Society.

Davies T. T., Crenshaw M. A. and Heatfield B. M. (1972) The effect of temperature on the chemistry and structure of echinoid spine regeneration. *J. Paleontol.* **46**(6), 874–883.

De Dekker P., Chivas A. R. and Shelley J. M. G. (1999) Uptake of Mg and Sr in the euryhaline ostracod *Cyprideis* determined from in vitro experiments. *Palaeogeogr. Palaeoclimatol. Palaeoecol.* **148**, 105–116.

Delaney M. L., Bé A. W. H. and Boyle E. A. (1985) Li, Sr, Mg, and Na in foraminiferal calcite shells from laboratory culture, sediment traps, and sediment cores. *Geochim. Cosmochim. Acta* **49**, 1327–1341.

DePaolo D. J. (2011) Surface kinetic model for isotopic and trace element fractionation during precipitation of calcite from aqueous solutions. *Geochim. Cosmochim. Acta* **75**, 1039–1056. https://doi.org/10.1016/j.gca.2010.11.020.

Detjen M., Sterling E. and Gómez A. (2015) Stable isotopes in barnacles as a tool to understand green sea turtle (*Chelonia mydas*) regional movement patterns. *Biogeosciences* **12**, 7081–7086. https://doi.org/10.5194/bg-12-7081-2015.

Dietzel M., Tang J., Leis A. and Köhler S. J. (2009) Oxygen isotopic fractionation during inorganic calcite precipitation – effect of temperature, precipitation rate and pH. *Chem. Geol.* **268**, 107–115. https://doi.org/10.1016/j.chemgeo.2009.07.015.

Dodd J. R. (1965) Environmental control of strontium and magnesium in *Mytilus*. *Geochim. Cosmochim. Acta* **29**, 385–398.

Dodd J. R. (1967) Magnesium and strontium in calcareous skeletons: a review. *J. Paleontol.* **41**(6), 1313–1329.

Dwyer G. S., Cronin T. M. and Baker P. A. (2002) Trace elements in marine ostracodes. In *The Ostracoda: Applications in Quaternary Research* (eds. A. R. Chivas and J. A. Holmes), pp. 205–225.

Emrich K., Ehhalt D. H. and Vogel J. C. (1970) Carbon isotope fractionation during the precipitation of calcium carbonate. *Earth Planet. Sci. Lett.* **8**, 363–371.

Epstein S., Buchsbaum R., Lowenstam H. A. and Urey H. C. (1953) Revised carbonate-water isotopic temperature scale. *Bull. Geol. Soc. Am.* **64**, 1315–1326.

Erez J. and Luz B. (1982) Experimental paleotemperature equation for planktonic foraminifera. *Geochim. Cosmochim. Acta* **47**, 1025–1031.

Foster B. A. (1987) Barnacle ecology and adaptation. *Crustaceana* **5**, 113–133.

Freitas P., Clarke L., Kennedy H., Richardson C. and Abrantes F. (2005) Mg/Ca, Sr/Ca, and stable isotope ($\delta^{18}O$ and $\delta^{13}C$) ratio profiles from the fan mussel *Pinna nobilis*: Seasonal records and temperature relationships. *Geochem. Geophys. Geosyst.* **6**(4). https://doi.org/10.1029/2004GC000872, Q04D14.

Freitas P. S., Clarke L. J., Kennedy H., Richardson C. A. and Abrantes F. (2006) Environmental and biological controls on elemental (Mg/Ca, Sr/Ca and Mn/Ca) ratios in shells of the king scallop *Pecten maximus*. *Geochim. Cosmochim. Acta* **70**, 5119–5133. https://doi.org/10.1016/j.gca.2006.07.029.

Freitas P. S., Clarke L. J., Kennedy H. and Richardson C. A. (2009) Ion microprobe assessment of the heterogeneity of Mg/Ca, Sr/Ca and Mn/Ca ratios in *Pecten maximus* and *Mytilus edulis* (bivalvia) shell calcite precipitated at constant temperature. *Biogeoscience* **6**, 1209–1227.

Gabitov R. I., Sadekov A. and Leinweber A. (2014) Crystal growth rate effect on Mg/Ca and Sr/Ca partitioning between calcite and fluid: an in situ approach. *Chem. Geol.* **367**, 70–82. https://doi.org/10.1016/j.chemgeo.2013.12.019.

Gal A., Weiner S. and Addadi L. (2015) A perspective on underlying crystal growth mechanisms in biomineralisation: solution mediated growth versus nanosphere particle accretion. *CrystEngComm* **17**, 2606. https://doi.org/10.1039/c4ce01474j.

Gale A. S. (2014) New thoracican cirripedes (Crustacea) from the Jurassic and Cretaceous of the UK. In Proceedings of the Geologists' Association, vol. 125, 406–418

Gale A. S. (2015) Phylogeny of the deep sea cirripede family Scalpellidae based on capitular plate morphology. *Zool. J. Linn. Soc.* **176**, 1–34.

Gale A. S. (2016) Origin and phylogeny of the thoracican cirripedes family Stramentidae. *J. Syst. Paleontol.* **14**(8), 653–702. https://doi.org/10.1080/14772019.2015.1091149.

Gale A.S. (2018) Stalked barnacles (Cirripedia, Thoracica) from the Late Jurassic (Tithonian) Kimmeridge Clay of Dorset, UK; palaeoecology and bearing on the evolution of living forms. In: Proceedings of the Geologists' Association, in press. https://dx.doi.org/10.1016/j.pgeola.2018.01.005.

Gale A. S. and Sørensen A. H. (2015) Cirripedia from the Campanian rocky shore at Ivo Klack, Sweden. *Cretac. Res.* **54**, 212–242. https://doi.org/10.1016/j.cretres.2014.09.004.

Gale A. S. and Schweigert G. (2016) A new phosphatic-shelled cirripedes (Crustacea, Thoracica) from the Lower Jurassic (Toarcian) of Germany – the oldest epiplanktonik barnacle. *Palaeontology* **59**(1), 59–70. https://doi.org/10.1111/pala.12207.

Gibbs P. E. and Bryan G. W. (1972) A study of strontium, magnesium, and calcium in the environment and exoskeleton of decapod crustaceans, with special reference to *Uca burgersi* on Barbuda, West Indies. *J. Exp. Mar. Biol. Ecol.* **9**, 97–110.

Gillikin D. P., Lorrain A., Navez J., Taylor J. W., André L., Keppens E., Baeyens W. and Dehairs F. (2005) Strong biological controls on Sr/Ca ratios in aragonitic marine bivalve shells. *Geochem. Geophys. Geosyst.* **6**(5), Q05009. https://doi.org/10.1029/2004GC000874.

Gordon C. M., Carr R. A. and Larson R. E. (1970) The influence of environmental factors on the sodium and manganese content of barnacle shells. *Limnol. Oceanogr.* **15**(3), 461–466.

Hermans J., Borremans C., Willenz P., André L. and Dubois P. (2010) Temperature, salinity and growth rate dependences of Mg/Ca and Sr/Ca ratios of the skeleton of the sea urchin *Paracentrotus lividus* (Lamarck): an experimental approach. *Mar. Biol.* **157**, 1293–1300. https://doi.org/10.1007/s00227-010-1409-5.

Hockett D., Ingram P. and LeFurgey A. (1997) Strontium and manganese uptake in the barnacle shell: electron probe microanalysis imaging to attain fine temporal resolution of biomineralisation activity. *Marine Environ. Res.* **43**(3), 131–143.

Iglikowska A., Ronowicz M., Humphreys-Williams E. and Kukliński P. (2018a) Trace element accumulation in the shell of the Arctic cirriped *Balanus balanus*. *Hydrobiologia* **818**, 43–56. https://doi.org/10.1007/s10750-018-3564-5.

Iglikowska A., Borszcz T., Drewnik A., Grabowska M., Humphreys-Williams E., Kędra M., Krzemińska M., Piwoni-Piórewicz A. and Kukliński P. (2018b) Mg and Sr in Arctic echinoderm calcite: nature or nurture? *J. Mar. Syst.* **180**, 279–288. https://doi.org/10.1016/j.jmarsys.2018.01.005.

Imai N., Terashima S., Itoh S. and Ando A. (1996) 1996 compilation of analytical data on nine GSJ geochemical reference samples, "sedimentary rock series". *Geostandards Newslett.* **20**(2), 165–216.

Ishimura T., Tsunogai U. and Nakagawa F. (2008) Grain-scale heterogeneities in the stable carbon and oxygen isotopic compositions of the international standard calcite materials (NBS 19, NBS 18, IAEA-CO-1, IAEA-CO8). *Rapid Commun. Mass Spectrom.* **22**, 1925–1932. https://doi.org/10.1002/rcm.3571.

Jacobs S. S., Fairbanks R. G. and Horibe Y. (1985) *Origin and Evolution of Water Masses Near the Antarctic Continental Margin: Evidence from $H_2^{18}O/H_2^{16}O$ Ratios in Seawater*. American Geophysical Union, pp. 59–85.

Jiménez-López C., Romanek C. S., Huertas F. J., Ohmoto H. and Caballero E. (2004) Oxygen isotope fractionation in synthetic magnesian calcite. *Geochim. Cosmochim. Acta* **68**(16), 3367–3377.

Killingley J. S. (1980) Migrations of California gray whales tracked by oxygen-18 variations in their epizoic barnacles. *Science* **207**, 759–760.

Killingley J. S. and Newman W. A. (1982) ^{18}O fractionation in barnacle calcite: a barnacle paleotemperature equation. *J. Mar. Res.* **40**(3), 893–902.

Killingley J. S. and Lutcavage M. (1983) Loggerhead turtle movements reconstructed from ^{18}O and ^{13}C profiles from commensal barnacle shells. *Estuar. Coast. Shelf Sci.* **16**, 345–349.

Kim S.-T. and O'Neil J. R. (1997) Equilibrium and nonequilibrium oxygen isotope effects in synthetic carbonates. *Geochim. Cosmochim Acta* **61**(16), 3461–3475.

Klein R. T., Lohmann K. C. and Thayer C. W. (1996) Sr/Ca and $^{13}C/^{12}C$ ratios in skeletal calcite of *Mytilus trossolus*: Covariation with metabolic rate, salinity, and carbon isotopic composition of seawater. *Geochim. Cosmochim. Acta* **60**(21), 4207–4221.

Mao Q., Shi P., Yin K., Gan J. and Qi Y. (2004) Tides and tidal currents in the Pearl River Estuary. *Cont. Shelf Res.* **24**, 1797–1808. https://doi.org/10.1016/j.csr.2004.06.008.

McConnaughey T. (1989a) ^{13}C and ^{18}O isotopic disequilibrium in biological carbonates: I. patterns. *Geochim. Cosmochim. Acta* **53**, 151–162.

McConnaughey T. (1989b) ^{13}C and ^{18}O isotopic disequilibrium in biological carbonates: II. *In vitro* simulation of kinetic isotope effects. *Geochim. Cosmochim. Acta* **53**, 163–171.

McConnaughey T. A., Burdett J., Whelan J. F. and Paull C. K. (1997) Carbon isotopes in biological carbonates: respiration and photosynthesis. *Geochim. Cosmochim. Acta* **61**(3), 611–622.

Milne A., Landing W., Bizimis M. and Morton P. (2010) Determination of Mn, Fe Co, Ni, Cu, Zn, Cd and Pb in seawater using high resolution magnetic sector inductively coupled mass spectrometry (HR-ICP-MS). *Anal. Chim. Acta* **665**, 200–207. https://doi.org/10.1016/j.aca.2010.03.027.

Morris A. W. (1974) Seasonal variation of dissolved metals in inshore waters of the Menai Straits. *Mar. Pollut. Bull.* **5**(4). https://doi.org/10.1016/0025-326X(74)90113-1, 54 49.

Nakamura R. and Tanaka M. (1995) Effects of aggregation on growth and survival of the intertidal stalked barnacle, *Capitulum mitella*. *Benthos Res.* **49**, 29–37.

Newman W. A. and Killingley J. S. (1985) The north-east Pacific intertidal barnacle *Pollicipes polymerus* in India? A biogeographical enigma elucidated by 18O fractionation in barnacle calcite. *J. Nat. Hist.* **19**(6), 1191–1196.

Odum H. T. (1951) The stability of the world strontium cycle. *Science* **114**, 407–411.

O'Neil J. R., Clayton R. N. and Mayeda T. K. (1969) Oxygen isotope fractionation in divalent metal carbonates. *J. Chem. Phys.* **51**(12).

Payne J. L., Heim N. A., Knope M. L. and McClain C. R. (2014) Metabolic dominance of bivalves predates brachiopod diversity decline by more than 150 million years. *Proc. Roy. Soc. B* **281**, 20133122. https://doi.org/10.1098/rspb.2013.3122.

Pérez-Huerta A., Cusack M., Jeffries T. E. and Williams C. T. (2008) High resolution distribution of magnesium and strontium and the evaluation of Mg/Ca thermometry in Recent brachiopod shells. *Chem. Geol.* **247**, 229–241. https://doi.org/10.1016/j.chemgeo.2007.10.014.

Pérez-Losada M., Harp M., Høeg J. T., Achituv Y., Jones D., Watanabe H. and Crandall K. A. (2008) The tempo and mode of barnacle evolution. *Mol. Phylogenet. Evol.* **46**, 328–346. https://doi.org/10.1016/j.ympev.2007.10.004.

Pilkey O. H. and Hower J. (1960) The effect of environment on the concentration of skeletal magnesium and strontium in *Dendraster*. *J. Geol.* **68**(2), 203–214.

Pilkey O. H. and Harriss R. C. (1966) The effect of intertidal environment on the composition of calcareous skeletal material. *Limnol. Oceanogr.* **11**(3), 381–385.

Pokroy B., Fitch A. N., Marin F., Kapon M., Adir N. and Zolotoyabko E. (2006) Anisotropic lattice distortions in biogenic calcite induced by intra-crystalline organic molecules. *J. Struct. Biol.* **155**, 96–103. https://doi.org/10.1016/j.jsb.2006.03.008.

Rathburn A. E. and De Dekker P. (1997) Magnesium and strontium composition of Recent benthic foraminifera from the Coral Sea, Australia and Prydz Bay, Antarctica. *Mar. Micropaleontol.* **32**, 231–248.

Reid D. G., Mason W. J., Chan B. K. K. and Duer M. J. (2012) Characterization of the phosphatic mineral of the barnacle *Ibla cumingi* at atomic level by solid-state nuclear magnetic resonance: comparison with other phosphatic biominerals. *J. R. Soc. Interface* **9**, 1510–1516.

Ries J. B. (2011) Skeletal mineralogy in a high-CO_2 world. *J. Exp. Mar. Biol. Ecol.* **403**, 54–64.

Schopf T. J. M. and Manheim F. T. (1967) Chemical composition of Ectoprocta (Bryozoa). *J. Paleontol.* **41**(5), 1197–1225.

Segev E. and Erez J. (2006) Effect of Mg/Ca ratio in seawater on shell composition in shallow benthic foraminifera. *Geochem. Geophys. Geosyst.* **7**(2), Q02P09. https://doi.org/10.1029/2005GC000969.

Shackleton N. J. (1974) Attainment of isotopic equilibrium between ocean water and the benthonic foraminifera genus Uvigerina: isotopic changes in the ocean during the last glacial. Collogues Internationaux du C.N.R.S. No 219.

Shanks A. L. (1986) Tidal periodicity in the daily settlement of intertidal barnacle larvae and an hypothesized mechanism for the cross-shelf transport of cyprids. *Biol. Bull.* **170**, 429–440.

Smith H. S., Delafontaine M. and Flemming B. W. (1988) Intertidal barnacles – assessment of their use as paleo-environment indicators using Mg, Sr, $^{18}O/^{16}O$, and $^{13}C/^{12}C$ variations. *Chem. Geol.* **73**, 211–220.

Swain G. W., Nelson W. G. and Preedeekanit S. (1998) The influence of biofouling adhesion and biotic disturbance on the development of fouling communities on non-toxic surfaces. *Biofouling* **12**(1–3), 257–269.

Tagliabue A. and Bopp L. (2008) Towards understanding global variability in ocean carbon-13. *Glob. Biogeochem. Cycles* **22**. https://doi.org/10.1029/2007GB003037, GB1025.

Tanaka N., Monaghan M. C. and Rye D. M. (1986) Contribution of metabolic carbon to mollusc and barnacle shell carbonate. *Nature* **320**, 520–523.

Tang J., Köhler S. and Dietzel M. (2008) Sr^{2+}/Ca^{2+} and $^{44}Ca/^{40}Ca$ fractionation during inorganic calcite formation: I. Sr incorporation. *Geochim. Cosmochim. Acta* **72**, 3718–3732. https://doi.org/10.1016/j.gca.2008.05.031.

Tarutani T., Clayton R. N. and Mayeda T. K. (1969) The effect of polymorphism and magnesium substitution on oxygen isotope fractionation between calcium carbonate and water. *Geochim. Cosmochim. Acta* **33**, 987–996.

Taubner I., Böhm F., Eisenhauer A., Garbe-Schönberg D. and Erez J. (2012) Uptake of alkaline earth metals in Alcyonarian spicules (Octocorallia). *Geochim. Cosmochim. Acta* **84**, 239–255. https://doi.org/10.1016/j.gca.2012.01.037.

Tesoriero A. J. and Pankow J. F. (1996) Solid solution partitioning of Sr^{2+}, Ba^{2+}, and Cd^{2+} to calcite. *Geochim. Cosmochim. Acta* **60**(6), 1053–1063.

Ullmann C. V. and Korte C. (2015) Diagenetic alteration in low-Mg calcite from macrofossils: a review. *Geol. Quart.* **59**(1), 3–20. https://doi.org/10.7306/gq.1217.

Ullmann C. V. and Pogge von Strandmann P. A. E. (2017) The effect of shell secretion rate on Mg/Ca and Sr/Ca ratios in biogenic calcite as observed in a belemnite rostrum. *Biogeosciences* **14**, 89–97. https://doi.org/10.5194/bg-14-89-2017.

Ullmann C. V., Campbell H. J., Frei R., Hesselbo S. P., Pogge von Strandmann P. A. E. and Korte C. (2013a) Partial diagenetic overprint of Late Jurassic belemnites from New Zealand: implications for the preservation potential of δ^7Li values in calcite fossils. *Geochim. Cosmochim. Acta* **120**, 80–96. https://doi.org/10.1016/j.gca.2013.06.029.

Ullmann C. V., Böhm F., Rickaby R. E. M., Wiechert U. and Korte C. (2013b) The Giant Pacific Oyster (*Crassostrea gigas*) as a modern analog for fossil ostreoids: Isotopic (Ca, O, C) and elemental (Mg/Ca, Sr/Ca, Mn/Ca) proxies. *Geochem. Geophys. Geosyst.* **14**(10), 4109–4120. https://doi.org/10.1002/ggge.20257.

Ullmann C. V., Hesselbo S. P. and Korte C. (2013c) Tectonic forcing of Early to Middle Jurassic seawater Sr/Ca. *Geology* **41** (12), 1211–1214. https://doi.org/10.1130/G34817.1.

Ullmann C. V., Frei R., Korte C. and Lüter C. (2017) Element/Ca, C and O isotope ratios in modern brachiopods: species-specific signals of biomineralisation. *Chem. Geol.* **460**, 15–24. https://doi.org/10.1016/j.chemgeo.2017.03.034.

Vander Putten E., Dehairs F., Keppens E. and Baeyens W. (2000) High resolution distribution of trace elements in the calcite shell layer of modern *Mytilus edulis*: environmental and biological controls. *Geochim. Cosmochim. Acta* **64**(6), 997–1011.

Vann C. D., Cronin T. M. and Dwyer G. S. (2004) Population ecology and shell chemistry of a phytal ostracode species (*Loxoconcha matagordensis*) in the Chesapeake Bay watershed. *Mar. Micropaleontol.* **53**, 261–277.

Wefer G. and Berger W. H. (1991) Isotope paleontology: growth and composition of extant calcareous species. *Mar. Geol.* **100**, 207–248.

Associate editor: Daniel Sinclair